Synchronisation of two chaotic delay differential systems

James Ong

This thesis is presented for the degree of
Masters of Science
of The University of Western Australia
Department of Mathematics & Statistics.
March 24, 2002

Abstract

The synchronisation of chaotic systems is a research area that has recently found application in the development of communication systems. In this thesis, Lyapunov functionals are used to gain insight into synchronisation, by the study of stability of the error system around zero. Two specific laser systems are given as examples, to show how well-established stability results extend to the area of synchronisation, and to highlight possible problems with this approach.

Contents

Acknowledgements

First and foremost, I would like to thank my supervisor, Prof. Alistair Mees, for his support, ideas and valuable time. I would also like to thank Dr. Gary Froyland and Dr. Kevin Judd who have supervised me for the last few months, while Alistair has been overseas.

Next, I would like to thank the other members of the Centre for Applied Dynamics and Optimisation (Dr. Berndt Pilgram, Dr. David Walker, and my fellow postgrads, David Allingham, Monty Craine, Yoshito Hirata, Devin Kilminster, Ronald Monson, Tomomichi Nakamura, David Ridout) for their ideas, criticism and help. While I have been at UWA, CADO has been an active research group which has been an inspiration to me in many ways.

Various overseas contacts need acknowledgement. The problem that I have been working on was supplied by various members of the Institute of Nonlinear Science at the University of California, San Diego, and so I have needed to consult with them to clarify details important to my analysis. In particular, I would like to thank Prof. Henry Abarbanel, Dr. Matt Kennel, and postgrads Mike Buhl and Lucas Illing for their time and feedback on my working papers. I would also like to thank postgrad student Shuo Tang at the University of California, Los Angeles, who has showed much interest in my research and provided an insight into realistic values for the semiconductor laser system.

I would like to thank the University of Western Australia for providing a scholarship to allow me to devote myself to this research degree.

I would like to thank my friends, especially Kat and Clare, who have, at times, lent me the strength to continue with my research, while always believing in me.

Lastly, I would like to thank my family and Robyn, for supporting my move to Western Australia.

Dedication

This thesis is dedicated to my father, who has always believed that I was able to achieve great things, and to Robyn, who endured my absence with remarkable resilience and grace.

Introduction

1.1 Background

At present, the use of chaotic dynamical systems to enhance communications systems is an active research area. There are a number of reasons that the use of chaos seems to be well suited to communications, at least at first glance. Firstly, signals produced and processed by chaotic systems are inherently broadband in nature. Broadband signals theoretically allow us to add various desirable properties to our system, including robustness to noise or avoidance of noisy frequency channels. We also have the ability to more efficiently optimise important statistical properties like peak signal power, since we are less constrained by bandwidth considerations. Secondly, chaotic signals may be high-dimensional, making long-term behaviour difficult to predict. This gives us the ability to incorporate encryption into our communications system.

In many proposed communication systems, there is a need for at least two chaotic signal generators, where the simplest type of system has one signal generator in the transmitter and an almost identical one in the receiver. The transmitting and receiving signal generator typically need to be synchronised to allow a message to be extracted from the transmitted signal. Synchronisation of the two chaotic systems needs to be robust to noise in the transmitted signal, as well as small differences between the two systems. In numerical simulations and experiments, there has been remarkable success in obtaining good synchronisation, even with relatively low levels of coupling between the systems, suggesting that synchronisation should be a robust process.

1.2 Communication system coupling schema

A basic communications system has a transmitter, a receiver and some type of communications channel between the two, allowing the transfer of information. It is desirable to have a communications schema that allows robustness to noise and loss of signal power, and the possibility of encryption of the signal.

In both of the systems to be featured in this thesis, optical feedback lasers are used as the transmitting and receiving systems. Theoretically, the transmitter and receiver should be almost identical. In an optical feedback laser, the output of the laser is fed back into the input of the laser by a fibre-optic cable. A one-way fibre optic cable joins the transmitter (drive system) and receiver (response system), with a special additive coupling feeding the driving signal into the feedback cable of the response system. Figure 1.2.1 shows a schematic of this set-up.

In a practical implementation of a feedback laser system of this kind, the fibre optic cable used to provide optical feedback is short (up to a few metres), while the fibre optic cable connecting the two systems could be hundreds of kilometres long. The carrier frequency may be in the terahertz range, while the message will be encoded more slowly; the best possible performance at present is probably in the gigahertz range. VanWiggeren and Roy [13] have successfully transmitted a 10 MHz message through a coupled set of chaotic lasers where the carrier had a wavelength

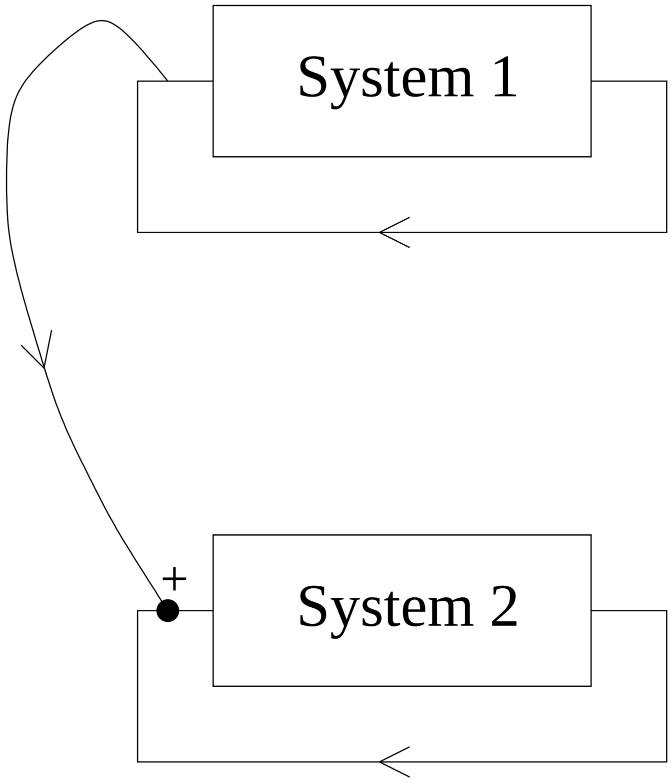

Figure 1.2.1: Schema of a communications system using feedback lasers

of about 1.53μm (equivalent to about 200 THz). With such high frequencies, synchronisation of phase in the carrier signal of the two systems is likely to be difficult, and thus should not be required for successful message transfer; synchronisation of the intensity of light produced by the systems should be sufficient. The two systems should also have similar internal states, so that the internal dynamics produce similar changes in intensity with time.

1.3 Outline of mathematical analysis

The mathematical analysis that forms the main part of this thesis allows us to study synchronisation of both the intensity variable and a variable derived from the population inversion, which is an internal state variable of a laser. The method of Lyapunov functions has been used to allow for slight differences between the drive and response system, as well as small amounts of noise in the communications channel. A valid Lyapunov function also gives us the guarantee that synchronisation is not lost once it is achieved. This is important because Heagy, Pecora and Carroll [7] have experimentally found synchronisation manifolds riddled with fractal holes, where synchronisation can be lost once it has been achieved.

The range of coupling that gives synchronisation may initially seem to be a strange parameter to investigate. After all, a complete coupling mathematically is more likely to produce more exact and robust synchronisation than partial coupling. However, partial coupling is more useful in practice than full coupling since the dynamics of the receiver system may help to reduce artifacts caused by noise in the communications channel.

The more difficult problem of message transfer between the two systems has not been studied in this thesis, since our analysis only ends up giving us meaningful results when the error between the two systems is close to zero. The amplitude of the message may be too large for our analysis, causing the error between the two systems to fall outside the domain of our results. However, if the message has a low energy compared to the carrier, it is possible that some generalisation may be drawn from our work to the case where there is a transmitted message.

1.4 Previous work

1.4.1 General results on robust synchronisation In this general area of synchronisation, many papers have tried to look at synchronisation as a type of feedback control, since in many ways, synchronisation is identical to the observer problem in control theory [11]. This approach is useful for some applications, like designing appropriate receivers for certain types of dynamical system or encryption regime. However, it seems that this approach fails to give us insight into stability for generic nonlinear time-varying systems.

A number of authors have noted that robust synchronisation is equivalent to uniform asymptotic stability of the error system around the zero solution. This insight has allowed application of standard results regarding uniform asymptotic stability that were initially developed by Lyapunov, and extended by Krasovskii [8] and other researchers to time delay systems.

Pecora and Carroll [9] showed that it is experimentally possible to synchronise two chaotic systems that are reasonably similar by using a master-slave coupling. They also mention that a necessary condition for synchronisation can be obtained just by studying the Lyapunov exponents of the error system. A later paper by the same authors [10] gives us the following theorem from Willems [14]:

Theorem 1. *The null solution of the nonlinear non-stationary system*

$$\dot{x} = A(t)x + h(x,t)$$

with $h(0,t) = 0$ for all t, is uniformly asymptotically stable if:

- $$\lim_{\|x\| \to 0} \frac{\|h(x,t)\|}{\|x\|} = 0$$

  holds uniformly with respect to t; this means that for any given positive δ, there must be a positive ϵ, independent of t, such that

  $$\frac{\|h(x,t)\|}{\|x\|} < \delta$$

  holds for all t and all $\|x\| < \epsilon$

- *$A(t)$ is bounded for all t*

- *the null solution of the linear system*

  $$\dot{x} = A(t)x$$

  is uniformly asymptotically stable.

This theorem gives us some conditions under which negative conditional Lyapunov exponents are sufficient for uniform asymptotic stability. These conditions basically say that if the nonlinear system is well-approximated by the linear system, an analysis of the linear system is sufficient. However, a direct application of this theorem for our two laser systems is difficult, since the equations cannot easily be put into the correct form.

Curran and Chua [5] use Lyapunov functions to develop a generic schema for testing synchronisation, but fail to consider time-delay systems. More useful is the paper by Pyragas [12], where he proved synchronisation with a pair of coupled Mackey-Glass systems using Lyapunov functions, and provided a starting point for the analysis in this thesis.

1.4.2 Previous results specific to our laser systems Previously, Abarbanel and Kennel [1] studied synchronisation of their Ikeda ring laser systems by calculating the largest conditional Lyapunov exponent of the error system, following the example of Pecora and Carroll [9]. They found that soon after the largest conditional Lyapunov exponent became negative, their numerical simulations demonstrated synchronisation in a reasonable time.

In addition to these numerical results, Abarbanel and Kennel analytically proved synchronisation for their system of coupled Ikeda ring lasers for complete coupling. However, as far as this author is aware, no other analytic work specific to these laser systems has been attempted.

Lyapunov functions

Lyapunov (or Liapunov) functions are a well-known tool to prove stability of a flow around an asymptotically stable equilibrium point. They allow us to guarantee stability of the equilibrium point even when the system is perturbed, as well as giving us a method to determine an estimate of the size of the basin of attraction. A good introduction to the concept is given in Hale and Koçak [6].

The concept of Lyapunov functions was extended to apply to differential systems with time-delay by Krasovskiĭ [8]. Krasovskiĭ's book comprehensively develops the theory of Lyapunov functions, and seems to be the key reference, as every book on delay differential equations or functional differential equations invariably cites it.

In this chapter, I will briefly introduce the concept of Lyapunov functions, and then outline the details necessary for the extension to delay differential systems. At the end, there is a section showing how stability for a simple delay differential equation is proven using a Lyapunov functional, giving us a template for more complicated systems of equations.

2.1 Introduction to Lyapunov functions

This section is intended to remind the reader of the fundamental concepts underlying the use of Lyapunov functions. For more detailed expositions, the reader is invited to read Hale and Koçak [6], from which key results for this section were taken, or to find a standard dynamics text, which is likely to mention the method of Lyapunov functions.

Definition (Positive definite). Let U be a neighborhood of $\mathbb{R}^2$ around the origin. A real-valued C^1 function $V : U \to \mathbb{R}$ given by $V(x),\ x \in \mathbb{R}^2$ is called positive definite on U if

(i) $V(0) = 0$;

(ii) $V(x) > 0$ for all $x \in U \setminus \{0\}$.

A function V is called *negative definite* if $-V$ is positive definite.

We now want to define the concepts of stability and asymptotic stability for the system

$$\dot{x} = f(x) \tag{2.1.1}$$

Definition (Stability). An equilibrium point $\bar{x}$ of system 2.1.1 is said to be stable if, for any given $\epsilon > 0$, there is a $\delta > 0$, depending on ϵ, such that, for every x_0 for which $|x_0 - \bar{x}| < \delta$, the solution $\varphi(t, x_0)$ of system 2.1.1 through x_0 at 0 satisfies the inequality $|\varphi(t, x_0) - \bar{x}| < \epsilon$ for all $t \geq 0$. The equilibrium point $\bar{x}$ is said to be unstable if it is not stable.

Definition (Asymptotic stability). An equilibrium point $\bar{x}$ is said to be asymptotically stable if it is stable and, in addition, there is an $r > 0$ such that $|\varphi(t, x_0) - \bar{x}| \to 0$ as $t \to +\infty$ for all x_0 satisfying $|x_0 - \bar{x}| < r$.

These definitions say that if the equilibrium solution $\bar{x}$ is stable and if our initial condition is close enough to it, then our solution x will stay in a ball around the equilibrium point for $t \geq 0$. If the null solution is asymptotically stable, then it is stable and in addition, $x - \bar{x}$ tends to zero whenever the initial condition is close enough to $\bar{x}$.

Theorem 2 (Lyapunov). *Let $\bar{x} = 0$ be an equilibrium point of $\dot{x} = f(x)$ and V be a positive definite C^1 function on a neighborhood U of 0.*

(i) If $\dot{V}(x) \leq 0$ for $x \in U \setminus \{0\}$, then 0 is stable.

(ii) If $\dot{V}(x) < 0$ for $x \in U \setminus \{0\}$, then 0 is asymptotically stable.

(iii) If $\dot{V}(x) > 0$ for $x \in U \setminus \{0\}$, then 0 is unstable.

Definition (Lyapunov function). A positive definite function V on an open neighborhood U of the origin is said to be a Lyapunov function for $\dot{x} = f(x)$ if $\dot{V} \leq 0$ for all $x \in U \setminus \{0\}$. When $\dot{V} < 0$ for all $x \in U \setminus \{0\}$, the function V is called a strict Lyapunov function.

We can see the idea behind the theorem by taking a Lyapunov function V and writing

$$\begin{aligned} \dot{V}(x) &= \nabla V(x) \cdot f(x) && (2.1.2) \\ &= \|\nabla V(x)\| \|f(x)\| \cos\theta && (2.1.3) \end{aligned}$$

where θ is the angle between $\nabla V(x)$ and $f(x)$. Note that $\dot{V}(x)$ has the sign of $\cos\theta$, and that $\nabla V(x)$ is normal to the level set containing x and points in the direction of increasing V. Also note that the level sets of V are closed curves. We can now say the following:

- If $\dot{V}(x) < 0$, $f(x)$ points inside the level set
- If $\dot{V}(x) > 0$, $f(x)$ points outside the level set
- If $\dot{V}(x) = 0$, $f(x)$ is tangential to the level set

Thus if $\dot{V}(x) < 0$ for all $x \in U \setminus \{0\}$, then all flow vectors must point inside respective level sets, meaning that the origin must be asymptotically stable, with U a subset of its basin of attraction.

The simplest function to use as a Lyapunov function is a quadratic form. This choice of Lyapunov function makes calculations simple if it works. In the cases where this choice does not work, there may be another obvious choice, which may be inspired by an energy function. However, it is not uncommon to find a system where all obvious choices fail to give us useful stability information. We come up against one of the serious limitations of the method of Lyapunov: that of finding a function that will satisfy all the necessary conditions.

2.2 Adaptation to equations with time delay

2.2.1 Basic framework of a delay differential system We are interested in considering a system of equations of the following form:

$$\frac{dx_i}{dt} = X_i\left(x_1(t), \ldots, x_n(t), x_1(t+\theta), \ldots, x_n(t+\theta), t\right) \tag{2.2.1}$$

This is a differential equation in terms of the current value of the state variable, the value of the state variable at time τ ago, and time. The initial condition for a delay differential system needs to be specified as a function of time, since we are working with an infinite-dimensional system. We will denote this function as $x_0(\theta_0)$, where $-h \leq \theta_0 \leq 0$. Note that θ_0 is reserved to parametrise our initial condition; if we want to parametrise x over the time period $t-h$ to t, we will write $(x(\theta))(t)$ where

$$(x(\theta))(t) = x(t+\theta), \quad -h \leq \theta \leq 0.$$

We would like to stabilise this system around the null solution $x = 0$, and would like the stable equilibrium to persist under a small perturbation. Krasovskiĭ [8] allows us to consider perturbations of the following form:

$$\begin{aligned} \frac{dx_i}{dt} \quad = \quad & X_i\left(x_1(t), \ldots, x_n(t), x_1(t-h_{i1}(t)), \ldots, x_n(t-h_{in}(t)), t\right) \\ & + R_i\left(x_1(t), \ldots, x_n(t), x_1(t-g_{i1}(t)), \ldots, x_n(t-g_{in}(t)), t\right)\right) \end{aligned} \tag{2.2.2}$$

where $0 \leq h_{ij}(t) \leq h,\ 0 \leq g_{ij}(t) \leq h$ for $i, j = 1, \ldots, n$, and R is 'small' in some sense. Note that this will allow for some mismatch in time-delay between our two systems, as well as mismatch in the state variable x.

2.2.2 Stability results It will be useful to define the h-norm that Krasovskiĭ uses as the standard functional norm in his analysis:

Definition (h-norm). The h-norm is defined as follows:

$$\|x\|^{(h)} = \sup_{\theta \in [-h, 0]} |x(\theta)|$$

We need to extend the concept of a positive definite function into this infinite-dimensional space; the following are taken from Definition 30.1 in Krasovskiĭ:

Definition (Positive definite). The functional $V(x_1(\theta), \ldots, x_n(\theta), t)$, defined for the vector functions $\{x_1(\theta), \ldots, x_n(\theta)\}$, $-h \leq \theta \leq 0$, for the region

$$\|x(\theta)\| < H,\ t \geq 0$$

is called positive definite in this region if there is a continuous function $w(r)$ that satisfies the conditions

$$\begin{aligned} & V(x_1(\theta), \ldots, x_n(\theta), t) \geq w\big(\|x(\theta)\|^{(h)}\big) \\ & w(r) > 0 \text{ for } r \neq 0 \end{aligned}$$

Definition (Infinitely small upper bound). The previously defined positive definite functional $V(x_1(\theta), \dots, x_n(\theta), t)$ has an infinitely small upper bound in the space

$$\|x(\theta)\| < H, \ t \geq 0$$

if there is a continuous function $W(r)$ satisfying the conditions

$$\begin{aligned} &V(x_1(\theta), \dots, x_n(\theta), t) \leq W\big(\|x(\theta)\|^{(h)}\big) \\ &W(0) = 0 \end{aligned}$$

The following two definitions are found combined as Definition 28.1 in Krasovskiĭ. They restate our definitions of stability and asymptotic stability in the context of Krasovskiĭ's framework.

Definition (Stability). The solution $x = 0$ of system (2.2.1) is called stable if for every positive number $\varepsilon > 0$ we can find a positive number $\delta > 0$ such that whenever the inequality

$$\|x_0(\theta_0)\|^{(h)} \leq \delta(\varepsilon, t_0)$$

is satisfied, the relation

$$\|x(x_0(\theta_0), t_0, t)\| < \varepsilon$$

holds for $t \geq t_0$

Definition (Asymptotic stability). The solution $x = 0$ of system (2.2.1) is asymptotically stable if it is stable and the conditions

$$\lim_{t \to \infty} \|x(x_0(\theta_0), t_0, t)\| = 0$$

$$\|x(x_0(\theta_0), t_0, t)\| < H_1 \text{ for all } \ t \geq t_0 \quad (H_1 = \text{const})$$

are satisfied for all initial curves $x_0(\theta_0)$ satisfying the inequality

$$\|x_0(\theta_0)\|^{(h)} \leq H_0 \quad (H_0 = \text{const})$$

(which specifies a region lying in the region of attraction of the unperturbed motion)

To paraphrase the definitions, if the null solution $x = 0$ is stable and if our initial condition is close enough to zero, then our solution $x(t)$ will stay in a ball around the origin for $t \geq t_0$. If the null solution is asymptotically stable, then it is stable and in addition, $x(t)$ tends to zero whenever the initial condition is close enough to zero.

We need a stronger concept than asymptotic stability to guarantee stability of the perturbed system. The following definition is found as Definition 30.2 in Krasovskiĭ.

Definition (Uniform asymptotic stability). The solution $x = 0$ of system (2.2.1) is called uniformly asymptotically stable with respect to the time $t_0 \geq 0$ and with respect to the initial curve $x_0(\theta_0)$ in region

$$\|x_0(\theta_0)\|^{(h)} \leq H_0$$

if it is asymptotically stable and also satisfies the following conditions:

- the number $\delta(\varepsilon) > 0$ in the definition of stability may be chosen independent of $t_0 \geq 0$
- for arbitrary $\eta > 0$, there exists a number $T(\eta)$ such that

  $$\|x(x_0(\theta_0), t_0, t + \theta)\|^{(h)} < \eta$$

  holds for every $t \geq t_0 + T(\eta)$, independent of the choice of a piecewise-continuous initial curve $x_0(\theta_0)$ in the region

  $$\|x_0(\theta_0)\|^{(h)} \leq H_0$$

Uniform asymptotic stability enforces asymptotic stability and guarantees that the rate of convergence to zero does not reduce to zero as t_0 increases. It also ensures that the synchronisation error converges to zero for *every* initial curve in a finite region – this precludes desynchronisation due to unstable orbits approaching infinitesimally close to the synchronisation manifold.

The following example (taken from Burton [4]) shows how a system can be asymptotically stable, but not uniformly asymptotically stable.

Example 1. Let $a : [0, \infty) \to \mathbb{R}$ be continuous and let

$$\dot{x} = a(t)x$$

where

- $a(n) = 0$ for each $n \in \mathbb{Z}^+$,
- $a(t) > 0$ for $2n < t < 2n + 1$,
- $a(t) < 0$ for $2n + 1 < t < 2n + 2$,
- $\int_{2n}^{2n+1} a(t)dt + \int_{2n+2}^{2n+3} a(t)dt = \int_{2n+1}^{2n+2} -a(t)dt$,
- $\int_{2n}^{2n+1} a(t)dt \to \infty$ as $n \to \infty$.

Then $x = 0$ is asymptotically stable, since the negative part of $a(t)$ forces $x(t)$ to zero. However, $x = 0$ is not uniformly asymptotically stable. To see this, set $t_0 = 2m$ where $m \in \mathbb{Z}^+$. Let us have a look at what happens in the time period $2m \leq t \leq 2m + 1$. If we solve the differential equation, we get

$$x(t) = x(t_0)e^{\int_{t_0}^{t} a(t)dt}.$$

With a fixed $x(t_0)$, $x(t_0+1)$ increases as t_0 increases. Thus, our initial condition $x(t_0)$ needs to be constrained to a smaller and smaller region around the origin (i.e. δ in the definition of stability needs to tend to zero) if we want $\|x\| < \epsilon$ for some fixed ϵ.

In Definition 32.1, Krasovskiĭ defines stability for persistent disturbances, which is exactly the sort of stability we need. It reads

Definition (Stable for persistent disturbances). The null solution of system (2.2.1) is called stable for persistent disturbances if for every $\varepsilon > 0$ there exist positive numbers δ_0, η, Ξ such that the solution $x(x_0(\theta_0), t_0, t)$ of the perturbed system (2.2.2) satisfies the inequality

$$\|x(x_0(\theta_0), t_0, t)\| < \varepsilon$$

for all $t \geq t_0, t_0 \geq 0$, whenever the initial curve $x_0(\theta_0)$ satisfies the inequality

$$\|x_0(\theta_0)\|^{(h)} \leq \delta_0$$

and the perturbed time delays h_{ij} and the functions R_i satisfy the inequalities

$$|R_i(x_1, \dots, x_n, y_1, \dots, y_n, t)| < \eta \quad (i = 1, \dots, n)$$

for $\|x\| < \varepsilon, \|y\| < \varepsilon$, and

$$|\tau - h_{ij}(t)| < \Xi \quad (i, j = 1, \dots, n)$$

The next theorem is found as Theorem 32.1 in Krasovskiĭ.

Theorem 3. *Suppose that the null solution $x = 0$ of equation (2.2.1) is uniformly asymptotically stable with respect to time t_0 and the initial curve $x_0(\theta_0)$. Then the null solution $x = 0$ is stable for persistent disturbances.*

This tells us that the study of uniform asymptotic stability tells us all we need to know about stability of a system under small perturbation (a perturbation of size at most η), even when the perturbation does not necessarily diminish with time. Another way of interpreting this result is as follows: we can keep synchronisation error less than a benchmark level if the null solution is stable for persistent disturbances, and the perturbation is never larger than a certain value.

2.2.3 Generalised Lyapunov functionals Krasovskiĭ states the following key theorem (found as Theorem 30.1) allowing us to apply the method of Lyapunov functions to systems of equations with time delay.

Theorem 4. *If to a differential equation (2.2.1) with time delay there corresponds a functional $V(x(\theta), t)$ which is positive definite in region*

$$\|x(\theta)\| < H$$

and has an infinitely small upper bound, and if the value

$$\limsup_{\Delta t \to +0} \left(\frac{V(x(x_0(\theta_0), t_0, t + \Delta t + \theta), t + \Delta t) - V(x(x_0(\theta_0), t_0, t + \theta), t)}{\Delta t} \right)$$

is negative definite along equation (2.2.1), then the null solution $x = 0$ of equation (2.2.1) is uniformly asymptotically stable with respect to time t_0 and the initial curve $x_0(\theta_0)$. If, moreover, the condition

$$\inf[V \text{ for } \|x(\theta)\|^{(h)} = H_1] > \sup[V \text{ for } \|x(\theta)\|^{(h)} = H_0]$$

is satisfied, where $H_0 < H_1 < H$, then the region of initial curves

$$\|x_0(\theta_0)\|^{(h)} < H_0$$

lies in the region of attraction of the point $x = 0$.

The following theorem, found as Theorem 30.2 in Krasovskiĭ, assures us that a Lyapunov functional will exist in the neighbourhood of the origin if the system is uniformly asymptotically stable to the origin.

Theorem 5. *If the null solution $x = 0$ of system (2.2.1) is uniformly asymptotically stable with respect to time t_0 and the initial curve $x_0(\theta_0)$ in region*

$$\|x_0(\theta_0)\|^{(h)} \leq H_0$$

then there is a functional $V(x(\theta), t)$, defined on the curves

$$\|x(\theta)\|^{(h)} \leq H_0$$

for $t \geq 0$, positive definite, having an infinitely small upper bound in this region, and having, moreover, a right derivative $\frac{dV}{dt} = \lim_{\Delta t \to 0^+} \frac{\Delta V}{\Delta t}$ on the trajectory of system (2.2.1). The derivative $\frac{dV}{dt}$ is a negative definite functional in some region

$$\|x(\theta)\|^{(h)} \leq H_0$$

and the functional $V(x(\theta), t)$ satisfies a Lipschitz condition with respect to $x(\theta)$; that is,

$$|V(x''(\theta), t) - V(x'(\theta), t)| \leq K_0 \|x''(\theta) - x'(\theta)\|^{(h)}$$

2.2.4 Example of a generalised Lyapunov functional The standard Lyapunov function to try for an ordinary differential equation is a quadratic form in the variables that we want to show stability in. To test for asymptotic stability around the origin for a system like

$$\dot{x} = f(x)$$

we might try to use the Lyapunov function

$$V = x^2$$

which would give us

$$\dot{V} = 2xf(x)$$

If $\dot{V}$ was negative definite in some neighborhood of the origin, we would be able to say that the origin was asymptotically stable.

For delay differential equations, we would not only like to show asymptotic stability, but also guarantee that the norm over the time period $t - r$ to t (for some r) of the solution is decreasing. Thus, our Lyapunov functional will include the quadratic form to ensure asymptotic stability, as well as a term to guarantee that the time-averaged norm of the solution is always decreasing.

Burton [4] gives us some examples of appropriate Lyapunov functionals for simple delay differential equations. He also states that he is using a prototype of the form

$$V(t, x_t) = x^T A(t)x + \int_{t-h(t)}^{t} x^T(s)B(s)x(s)ds$$

to try to show uniform asymptotic stability for the origin for the system

$$\dot{x} = f(t, x_t)$$

where $x_t(s) = x(t+s)$. Note that the second part of the Lyapunov functional guarantees that the h-norm over the time period $t - h$ to t always decreases with increasing t.

Example 2. This simple example can be found as Example 4.2.6 in Burton.

$$\dot{x}(t) = -ax(t) + bx(t-h)$$

where a, b and h are positive constants and $a > b$. Let $t_0 \in \mathbb{R}$ and ϕ be the initial condition (specified over the domain $t_0 - h \leq t \leq t_0$). To simplify the notation, let us write $x(t)$ as x and $x(t-h)$ as x_h. Burton uses the following functional to show uniform asymptotic stability:

$$V(t, x_t) = x^2 + b\int_{t-h}^{t} x^2(s)ds$$

Differentiation gives us

$$\begin{aligned}
\dot{V}(t, x_t) &= 2x\dot{x} + b(x^2 - x_h^2) \\
&= 2x(-ax + bx_h) + bx^2 - bx_h^2 \\
&= -2ax^2 + bx^2 + b(-x^2 + 2xx_h - x_h^2) + bx^2 \\
&= -2ax^2 + 2bx^2 - b(x - x_h)^2 \\
&\leq (-2a + 2b)x^2 \leq 0
\end{aligned}$$

Now, we apply Theorem 4 to confirm that V is a valid Lyapunov functional:

- V is positive definite on $\|x(\theta)\| < H$ for all H since it is the sum of positive definite functions

- For $x(\theta) \neq 0$, $V \neq 0$ (assuming a continuous history function)

- $\dot{V}(t, x_t) \leq 0$, and $\dot{V}(t, x_t) = 0$ only when $x = x_h = 0$

This proves that the null solution is uniformly asymptotically stable. Since this is true for all H, then all points lie in the region of attraction of the null solution.

2.2.5 Choice of Lyapunov functional In some ways, the choice of Lyapunov functional is a rather arbitrary process. As long as the chosen function satisfies Theorem 4, the local stability of the null solution is proven. However, there are some factors to consider when choosing possible candidates for the Lyapunov function. Two factors that are important for this thesis are:

- Is the chosen candidate a valid Lyapunov function over the domain of the problem (and can this be proven analytically)?

- Can the candidate be generalised for use in other dynamical systems?

The first condition seems rather obvious. However, it is possible that one might find a candidate function by trial and error, and use numerical simulation to try to test whether it seems to be valid. This gives some insight, but by using these means alone, it is not possible to guarantee that the candidate is truly a Lyapunov function.

The second condition is the one that describes the value of the Lyapunov function to other researchers in the area. Of course, it is nice to be able to prove the existence of a Lyapunov function for a certain problem, but this approach would be of limited use if other researchers could not apply a similar candidate to a similar problem.

The following example shows the same dynamical system as in Example 2, but uses a different Lyapunov function to show stability of the null solution. This candidate Lyapunov function is a generalised form of the last one.

Example 3. We have the same system as before:

$$\dot{x} = -ax + bx_h$$

where a, b and h are positive constants and $a > b$. Let $t_0 \in \mathbb{R}$ and ϕ be the initial condition (specified over the domain $t_0 - h \leq t \leq t_0$). We will now use the following (generalised) functional to show uniform asymptotic stability:

$$V(t, x_t) = x^2 + \mu \int_{t-h}^{t} x^2(s) ds$$

Differentiation gives us

$$\begin{aligned}
\dot{V}(t,x_t) &= 2x\dot{x} + \mu(x^2 - x_h^2) \\
&= 2x(-ax + bx_h) + \mu x^2 - \mu x_h^2 \\
&= -2ax^2 + \mu x^2 + 2bxx_h - \mu x_h^2 \\
&= -2ax^2 + \mu x^2 + \left(-\left(\frac{b}{\sqrt{\mu}}\right)^2 x^2 + 2bxx_h - \mu x_h^2 \right) + \left(\frac{bx}{\sqrt{\mu}}\right)^2 \\
&= x^2\left(-2a + \mu + \frac{b^2}{\mu}\right) - \left(\frac{b}{\sqrt{\mu}}x - \sqrt{\mu}x_h\right)^2 \\
&\leq x^2\left(-2a + \mu + \frac{b^2}{\mu}\right)
\end{aligned}$$

Thus we can guarantee that $\dot{V} < 0$ when

$$-2a + \mu + \frac{b^2}{\mu} < 0$$

This is true when

$$\mu \in \left(a - \sqrt{a^2 - b^2}, a + \sqrt{a^2 - b^2}\right)$$

Note that Example 2, with $\mu = b$, was a special case of this example, since

$$a - \sqrt{a^2 - b^2} < b < a + \sqrt{a^2 - b^2}$$

when $a > b > 0$. The use of Theorem 4 is exactly the same as shown in Example 2.

This example shows that many functions of the same form serve as Lyapunov functions for our dynamical system. In one sense, the choice of $\mu = a$ can be thought of as the 'best' since it gives the most negative value for $\dot{V}$, and thus guarantees the quickest rate of convergence of the system to the null solution.

For systems where the basin of attraction of the null solution is not the whole space, a 'good' choice of Lyapunov function may be one that gives a reasonable estimate of the size of the basin of attraction. This ability to choose a Lyapunov function stems from the fact that Lyapunov functions give a sufficient, but not necessary, condition for stability. In other words, the existence of a Lyapunov function over a specified domain proves that all points in that domain will converge to the null solution, but does not preclude the existence of a larger basin of attraction.

In the following sections, we will use a similar Lyapunov function to the one Burton used, though tailored to our specific systems. The reader should bear in mind that there is likely to be a 'better' choice of function that gives less conservative estimates for the questions we need to answer, but that the time and effort to find or construct such a function may not give a worthwhile payoff.

Ikeda ring laser

In this chapter, we will apply the method of Lyapunov functions to a system of equations modelling coupled Ikeda lasers. We will find that this method gives us a conservative estimate of the amount of coupling needed to maintain robust synchronisation.

3.1 Abarbanel-Kennel laser system

Abarbanel and Kennel [1] model an experimental laser system (known as the Ikeda ring laser) in the following way:

$$\begin{aligned} \zeta(t+\tau) &= E_I e^{i(\omega_I-\omega_0)t} + Be^{i\kappa}\zeta(t)e^{(\beta+i\alpha)w(t)} \\ \dot{w}(t) &= Q - 2\gamma\left(w(t) + 1 + \frac{|\zeta(t)|^2(e^{Gw(t)}-1)}{G}\right) \end{aligned}$$

where ζ and w are the scalar variables. The complex electric field amplitude is ζ. The real spatially averaged population inversion is transformed in a simple way to give w. Note that this means that w can be negative. The physical constants and parameters are $E_I, \omega_I, \omega_0, B, \kappa, \beta, \alpha, Q, \gamma, G$.

This set of equations is a map and a differential equation, but Krasovskiĭ's analysis also holds for systems where the state variables depend on the entire history function:

$$\frac{dx_i}{dt} = X_i\left(x_1(t+\theta), \ldots, x_n(t+\theta), t\right)$$

where $i = 1, \ldots, n$ and $-h \le \theta \le 0$. Now note that if we differentiate the first equation, we get $\dot{\zeta}$ dependent on $\dot{\zeta}_\tau$, which is an implicit function of the history function around time $t-\tau$.

Let us use the notation $w_\tau(t) = w(t-\tau)$, $\zeta_\tau(t) = \zeta(t-\tau)$. If we assume that $\omega_I = \omega_0$, we get the equations

$$\zeta = f(w_\tau, \zeta_\tau) \tag{3.1.1}$$
$$\dot{w} = g(w, |\zeta|^2) \tag{3.1.2}$$

where

$$\begin{aligned} f(w_\tau, \zeta_\tau) &= E_I + \Lambda\zeta_\tau e^{\xi w_\tau} \\ g(w, |\zeta|^2) &= Q - 2\gamma\left(w + 1 + |\zeta|^2(e^{Gw}-1)/G\right) \end{aligned}$$

and $\xi = \beta + i\alpha$, $\Lambda = Be^{i\kappa}$. Note that $\dot{w}$ only depends on the size of ζ and not the phase.

Thus, the coupled system of Figure 1.2.1 has the following equations:

$$\begin{array}{lrcl} \text{System 1} & \zeta &=& f(w_\tau, \zeta_\tau) \\ & \dot{w} &=& g(w, |\zeta|^2) \\ \text{Coupling} & \zeta'' &=& K\zeta + (1-K)\zeta' \\ \text{System 2} & \zeta' &=& f(w'_\tau, \zeta''_\tau) \\ & \dot{w}' &=& g(w', |\zeta''|^2) \end{array}$$

The parameter K describes the strength of the coupling between the two laser systems, where $K = 0$ describes no coupling, while $K = 1$ describes complete coupling. Previously, Abarbanel and Kennel [1] proved global synchronisation for the case $K = 1$. This value is less useful in practice since it corresponds to inserting the transmitted signal directly into the receiver and throwing away the receiver's feedback loop which makes it more difficult for the receiver to compensate for corruption of the transmitted signal.

3.2 Application of Lyapunov function

Let $\Gamma = \zeta - \zeta'$ and $\Delta = w - w'$. A possible choice of Lyapunov function to show stability in the error system around the trivial solution is

$$V(t) = \frac{1}{2}\Delta(t)^2 + \mu_1 \int_{t-\tau}^{t} |\Gamma(\theta)|^2 d\theta + \mu_2 \int_{t-\tau}^{t} \Delta(\theta)^2 d\theta \tag{3.2.1}$$

where $\mu_1 > 0$, $\mu_2 > 0$. This choice allows us to study robust synchronisation of ζ and w over the entire time period $t - \tau$ to t. We have left out the term $\frac{1}{2}|\Gamma(t)|^2$ because we have no explicit information about $\dot{\zeta}$, and $\dot{V}(t)$ would require that information. It is also true that this term is not required when the history function is continuous, since forcing the integral term

$$\int_{t-\tau}^{t} |\Gamma(\theta)|^2 d\theta$$

to be monotone decreasing also forces $|\Gamma(t)|^2$ to be monotone decreasing.

We want to find equations that determine Γ and Δ. To make things simpler, we will start by linearising about the synchronised state. Observe that

$$\zeta - \zeta'' = (1 - K)\Gamma.$$

From (3.1.1),

$$\begin{aligned} \Gamma &= f(w_\tau, \zeta_\tau) - f(w'_\tau, \zeta''_\tau) \\ &\approx \partial_{w_\tau} f(w_\tau, \zeta_\tau)\Delta_\tau + (1-K)\partial_{\zeta_\tau} f(w_\tau, \zeta_\tau)\Gamma_\tau \\ &= \xi(\zeta - E_I)\Delta_\tau + (1-K)\Lambda e^{\xi w_\tau}\Gamma_\tau \end{aligned}$$

where Γ is complex.

From (3.1.2),

$$\begin{aligned} \dot{\Delta} &= g(w, |\zeta|^2) - g(w', |\zeta''|^2) \\ &\approx \partial_w g(w, |\zeta|^2)\Delta + \partial_{|\zeta|^2} g(w, |\zeta|^2)(|\zeta''|^2 - |\zeta|^2) \\ &= -2\gamma(1 + |\zeta|^2 e^{Gw})\Delta - (2\gamma/G)(e^{Gw} - 1)(|\zeta''|^2 - |\zeta|^2) \end{aligned}$$

where $\dot{\Delta}$ is real, and

$$\begin{aligned} |\zeta''|^2 - |\zeta|^2 &= \zeta''(\zeta'')^* - \zeta\zeta^* \\ &= (\zeta - (1-K)\Gamma)(\zeta^* - (1-K)\Gamma^*) - \zeta\zeta^* \\ &= -(1-K)(\zeta^*\Gamma + \zeta\Gamma^*) + (1-K)^2\Gamma\Gamma^*. \end{aligned}$$

3.3 Lyapunov stability using the linearised equations

Using the Lyapunov function proposed in (3.2.1) we get

$$\begin{aligned}\dot{V} &= \Delta\dot{\Delta} + \mu_1(|\Gamma|^2 - |\Gamma_\tau|^2) + \mu_2(\Delta^2 - \Delta_\tau^2) \\ &= -2\gamma(1+|\zeta|^2 e^{Gw})\Delta^2 \\ &\quad - (2\gamma\Delta/G)(e^{Gw}-1)\left[-(1-K)(\zeta^*\Gamma + \zeta\Gamma^*) + (1-K)^2\Gamma\Gamma^*\right] \\ &\quad + \mu_1\left(|\Gamma|^2 - |\Gamma_\tau|^2\right) + \mu_2(\Delta^2 - \Delta_\tau^2).\end{aligned}$$

The term involving $\Delta\Gamma\Gamma^*$ is third order and can be neglected to the present working accuracy. We aim to collect together the remaining terms, grouping them as coefficients of quadratics in Δ, Δ_τ, Γ and Γ_τ. Rewrite $\dot{V}$ as

$$\dot{V} = -|a\Delta + b\Gamma|^2 + |b\Gamma|^2 + \mu_1(|\Gamma|^2 - |\Gamma_\tau|^2) - \mu_2\Delta_\tau^2$$

where

$$a^2 = 2\gamma(1+|\zeta|^2 e^{Gw}) - \mu_2 \tag{3.3.1}$$

is positive real if μ_2 is small enough, and

$$ab = -2(1-K)\gamma(e^{Gw}-1)\zeta^*/G$$

so b is $O(1-K)$.

Next we substitute

$$|\Gamma|^2 = \left|\xi(\zeta - E_I)\Delta_\tau + (1-K)\Lambda e^{\xi w_\tau}\Gamma_\tau\right|^2$$

which we will write as

$$|\Gamma|^2 = |c\Delta_\tau + d\Gamma_\tau|^2$$

where d is $O(1-K)$. This gives

$$\begin{aligned}\dot{V} &= -|a\Delta + b\Gamma|^2 + (\mu_1 + |b|^2)\,|c\Delta_\tau + d\Gamma_\tau|^2 - \mu_1|\Gamma_\tau|^2 - \mu_2\Delta_\tau^2 \\ &= -|a\Delta + b\Gamma|^2 - |p\Delta_\tau + q\Gamma_\tau|^2 - (\mu_1 - |q|^2)|\Gamma_\tau|^2 + |d\Gamma_\tau|^2(\mu_1 + |b|^2)\end{aligned} \tag{3.3.2}$$

where

$$|p|^2 = \mu_2 - (\mu_1 + |b|^2)|c|^2 \tag{3.3.3}$$

is positive real if μ_2 is large enough, and

$$pq^* = -(\mu_1 + |b|^2)cd^*.$$

Thus, to make $\dot{V}$ negative definite, we require

$$\mu_2 < 2\gamma[(1+|\zeta|^2)e^{Gw}]_{\min} \tag{3.3.4}$$

$$\mu_2 > [(\mu_1 + |b|^2)|c|^2]_{\max} \tag{3.3.5}$$

$$\mu_1 > \left[\frac{|q|^2 + |db|^2}{1 - |d|^2}\right]_{\max} \tag{3.3.6}$$

which are respectively the condition (from equation 3.3.1) for a^2 to be positive real, the condition (from equation 3.3.3) for $|p|^2$ to be positive real, and the requirement (from equation 3.3.2) that the coefficient of $|\Gamma_\tau|^2$ in $\dot{V}$ be negative. Note that the subscripts min and max (used both here and later in this analysis) signify the respective minimum and maximum values taken over the entire domain of the problem, and as such are not time dependent. We will satisfy each of these conditions in order.

First, choose μ_2 to be ϕ times the right hand side of (3.3.4), where $\phi \in (0,1)$ since $\mu_2 > 0$. That is,

$$\mu_2 = 2\phi\gamma[(1+|\zeta|^2)e^{Gw}]_{\min}. \tag{3.3.7}$$

This choice of μ_2 makes

$$a^2_{\min} = 2(1-\phi)\gamma[(1+|\zeta|^2)e^{Gw}]_{\min}$$

and

$$|b|^2_{\max} = \frac{2(1-K)^2\gamma[(e^{Gw}-1)^2|\zeta|^2]_{\max}}{(1-\phi)G^2[(1+|\zeta|^2)e^{Gw}]_{\min}}. \tag{3.3.8}$$

Next, satisfy (3.3.5) by choosing μ_1 so that the right hand side (which by inspection is always positive) is $\theta\mu_2$ for some $\theta \in (0,1)$, to be determined. Thus

$$\mu_1 = \frac{\theta\mu_2}{|c|^2_{\max}} - |b|^2_{\max}. \tag{3.3.9}$$

We will investigate later the constraints placed upon K to keep μ_1 positive. This choice of μ_1 makes

$$\begin{aligned} |p|^2_{\min} &= \mu_2 - (\mu_1 + |b|^2_{\max})|c|^2_{\max} \\ &= (1-\theta)\mu_2. \end{aligned}$$

Finally we have to ensure that (3.3.6) holds. With our choice of μ_1 and μ_2, and using the above expression for $|p|^2_{\min}$,

$$\begin{aligned} |q|^2_{\max} &= \frac{(\mu_1 + |b|^2_{\max})|c|^2_{\max}|d|^2_{\max}}{|p|^2_{\min}} \\ &= \frac{(\mu_1 + |b|^2_{\max})|c|^2_{\max}|d|^2_{\max}}{(1-\theta)\mu_2} \\ &= \frac{\theta\mu_2|d|^2_{\max}}{(1-\theta)\mu_2} \\ &= \frac{\theta}{1-\theta}|d|^2_{\max}. \end{aligned}$$

Thus $|q|^2$ is order $(1-K)^2$, because $|d|^2$ is of that order. We require

$$\mu_1 > \left[\frac{|q|^2 + |db|^2}{1-|d|^2}\right]_{\max}$$

giving

$$\left[\frac{|d|^2\left(\frac{\theta}{1-\theta}+|b|^2\right)}{1-|d|^2}\right]_{\max} > 0. \tag{3.3.10}$$

We note that

$$\frac{\theta}{1-\theta}+|b|^2 > 0$$

since $\theta \in (0,1)$, so inequality 3.3.10 is equivalent to

$$\left[\frac{|d|^2}{1-|d|^2}\right]_{\max} > 0$$

Since

$$|d| = (1-K)|\Lambda|$$

and $0 \leq K \leq 1$, $|\Lambda| = 0.9$, this inequality is satisfied.

This leaves us with only one condition to satisfy: $\mu_1 > 0$. Substituting expressions for μ_2 and $|b|^2_{\max}$ from (3.3.7) and (3.3.8) into (3.3.9), and noting that

$$|c|^2_{\max} = |\xi|^2|\zeta - E_I|^2_{\max}$$

we get

$$\frac{2\theta\phi\gamma[(1+|\zeta|^2)e^{Gw}]_{\min}}{|\xi|^2|\zeta-E_I|^2_{\max}} - \frac{2(1-K)^2\gamma[(e^{Gw}-1)^2|\zeta|^2]_{\max}}{(1-\phi)G^2[(1+|\zeta|^2)e^{Gw}]_{\min}} > 0$$

To keep our analysis rigorous, we will strengthen this inequality (making the end result more conservative) by distributing the max and min qualifiers through each term. The stronger inequality is

$$\frac{2\theta\phi\gamma\left[(1+|\zeta|^2_{\min})e^{Gw_{\min}}\right]}{|\xi|^2|\zeta-E_I|^2_{\max}} - \frac{2(1-K)^2\gamma\left[[(e^{Gw}-1)^2]_{\max}|\zeta|^2_{\max}\right]}{(1-\phi)G^2\left[(1+|\zeta|^2_{\min})e^{Gw_{\min}}\right]} > 0$$

Using the fact that $K \leq 1$, and solving the quadratic inequality, we get

$$1-\sqrt{\frac{(1-\phi)\phi\theta G^2 e^{2Gw_{\min}}(1+|\zeta|^2_{\min})^2}{|\xi|^2|\zeta-E_I|^2_{\max}|\zeta|^2_{\max}[(e^{Gw}-1)^2]_{\max}}} < K \leq 1. \tag{3.3.11}$$

To get the maximum range for K, we set $\phi = 0.5$ and $\theta \approx 1$. Using values of

- ($|\Lambda| = 0.9$ as used previously in the analysis)
- $|\xi| = 6$
- $E_I = 1$

- $G = 0.01$
- $w_{\min} = -0.8292$
- $w_{\max} = 0$
- $|\zeta|_{\min} = 0$
- $|\zeta|_{\max} = 3.516$

we get the range

$$0.989 < K \leq 1$$

The values for parameters were taken from [1], while the values for the domain of w and $|\zeta|$ were obtained from Mike Buhl [3].

Thus we have shown that for all K sufficiently close to 1, $\dot{V}$ is negative definite in some open neighbourhood of $(\Delta = 0, \Delta_\tau = 0, \Gamma = 0, \Gamma_\tau = 0)$. Since V was defined so as to be positive definite, V is a strict Lyapunov functional for the origin in $(\Delta, \Delta_\tau, \Gamma, \Gamma_\tau)$ space and the origin is therefore uniformly asymptotically stable: that is, synchronisation is assured as long as the coupling constant K is close enough to 1 and the initial conditions are not too far from the synchronisation manifold.

Note that this analysis gives a very conservative estimate of the range of K for which coupling occurs, firstly because one of the inequalities was strengthened in a rather crude manner to allow analytical results, and secondly because we are using the method of Lyapunov functions, which give sufficient, but not necessary, conditions for synchronisation. Numerical calculation of the Lyapunov function while the system is evolving eliminates the need for linearisation (giving a larger estimate of the basin of attraction), as well as removing any approximations required for an analytic solution – both of these are good reasons to calculate the Lyapunov function numerically in simulations and experiments. However, it is important that the local stability of the null solution (perfect synchronisation) be shown analytically, to rule out a synchronisation manifold riddled with fractal holes [7] that may be difficult to detect in simulations or experiments.

Semiconductor laser

In this chapter, we will apply the method of Lyapunov functions to a system of equations modelling coupled semiconductors, and confront some of the difficulties involved with this method. We will gain some insight into synchronisation behaviour for this particular system, and present the hypothesis that robust synchronisation does not necessarily occur for this system.

4.1 Abarbanel-Kennel-Illing laser system

Abarbanel, Kennel and Illing [2] model an experimental laser system using

$$\begin{aligned} \dot{I} &= \frac{\gamma_C}{\gamma_S}\left[\frac{1+\frac{\gamma_N}{\gamma_S \mathcal{J}}n}{1+\frac{\gamma_P}{\gamma_C}(I-1)} - 1\right] I \\ \dot{n} &= \mathcal{J}\left[1 - \left(\frac{1+\frac{\gamma_N}{\gamma_S \mathcal{J}}n}{1+\frac{\gamma_P}{\gamma_C}(I-1)}\right) I\right] - n + \epsilon I_\tau \end{aligned}$$

where I and n are the real scalar variables, and $I_\tau(t) = I(t-\tau)$. The intensity is I. The spatially averaged population inversion is transformed in a simple way to give n. The physical constants and parameters are as follows:

- $\mathcal{J} = 0.6667$
- $\gamma_C = 2.4 \times 10^{11} s^{-1}$
- $\gamma_S = 1.458 \times 10^{9} s^{-1}$
- $\gamma_N = 1.333 \times 10^{9} s^{-1}$
- $\gamma_P = 2.4 \times 10^{9} s^{-1}$

The feedback parameter ϵ can be varied, and for the simulations has been set to 0.3. With this value of ϵ, numerical simulations show that I ranges between 0 and 11, while n ranges between -0.15 and 0.25.

Write the system in the form

$$\begin{aligned} \dot{I} &= f(I,n) \\ \dot{n} &= g(I,n,I_\tau) \end{aligned}$$

and couple it with a second system

$$\begin{aligned} \dot{I}' &= f(I',n') \\ \dot{n}' &= g(I',n',I''_\tau) \end{aligned}$$

via

$$I'' = KI + (1-K)I'$$

where K is the coupling constant, with $K = 0$ representing no coupling and $K = 1$ representing full coupling.

4.2 Lyapunov function

Define

$$\begin{aligned}\Gamma &= I' - I \\ \Delta &= n' - n \\ \Gamma_\tau &= I'_\tau - I_\tau\end{aligned}$$

We hope to have a valid Lyapunov function of the form

$$V = \frac{1}{2}\Gamma^2 + \frac{\lambda}{2}\Delta^2 + \mu \int_{t-\tau}^{t} \Gamma(\theta)^2 d\theta$$

because we want to study robust synchronisation of I over the time period $t-\tau$ to t (which is effectively the intensity everywhere in the feedback loop). Also note that we have no explicit information about n_τ which would be necessary if we wanted to include the time-delay integral of the error in population inversion. Differentiation of V gives

$$\dot{V} = \Gamma\dot{\Gamma} + \lambda\Delta\dot{\Delta} + \mu(\Gamma^2 - \Gamma_\tau^2) \tag{4.2.1}$$

4.3 Conditions arising from linearisation

$$\begin{aligned}\dot{\Gamma} &= f(I', n') - f(I, n) \\ \dot{\Delta} &= g(I', n', I''_\tau) - g(I, n, I_\tau)\end{aligned}$$

After linearisation, we have

$$\begin{aligned}\dot{\Gamma} &\approx \partial_I f(I,n)\Gamma + \partial_n f(I,n)\Delta \\ &= \left\{ \frac{\gamma_C}{\gamma_S}\left[\frac{1+\frac{\gamma_N}{\gamma_S \mathcal{J}}n}{1+\frac{\gamma_P}{\gamma_C}(I-1)} - 1\right] - \frac{\gamma_P}{\gamma_S} I \left[\frac{1+\frac{\gamma_N}{\gamma_S \mathcal{J}}n}{\left(1+\frac{\gamma_P}{\gamma_C}(I-1)\right)^2}\right]\right\}\Gamma \\ &\quad + \frac{\gamma_C\gamma_N}{\gamma_S^2 \mathcal{J}} \frac{I\Delta}{1+\frac{\gamma_P}{\gamma_C}(I-1)} \\ \dot{\Delta} &\approx \partial_I g(I,n,I_\tau)\Gamma + \partial_n g(I,n,I_\tau)\Delta + (1-K)\partial_{I_\tau} g(I,n,I_\tau)\Gamma_\tau \\ &= -\mathcal{J}\left\{\frac{1+\frac{\gamma_N}{\gamma_S \mathcal{J}}n}{1+\frac{\gamma_P}{\gamma_C}(I-1)} - \frac{\gamma_P}{\gamma_C}\left[\frac{I(1+\frac{\gamma_N}{\gamma_S \mathcal{J}}n)}{\left(1+\frac{\gamma_P}{\gamma_C}(I-1)\right)^2}\right]\right\}\Gamma \\ &\quad - \left[\frac{I\frac{\gamma_N}{\gamma_S}}{1+\frac{\gamma_P}{\gamma_C}(I-1)} + 1\right]\Delta + (1-K)\epsilon\Gamma_\tau\end{aligned}$$

Substituting this into (4.2.1), we get

$$\begin{aligned}
\dot{V} &= \Gamma^2 \left[\frac{\gamma_C}{\gamma_S} \left(\frac{1+\frac{\gamma_N}{\gamma_S \mathcal{J}} n}{1+\frac{\gamma_P}{\gamma_C}(I-1)} - 1 \right) - \frac{\gamma_P}{\gamma_S} I \left[\frac{1+\frac{\gamma_N}{\gamma_S \mathcal{J}} n}{\left(1+\frac{\gamma_P}{\gamma_S}(I-1)\right)^2} \right] + \mu \right] \\
&\quad + \Gamma\Delta \left[\frac{\gamma_C \gamma_N}{\gamma_S^2 \mathcal{J}} \frac{I}{1+\frac{\gamma_P}{\gamma_C}(I-1)} \right. \\
&\quad \left. - \frac{\lambda \mathcal{J} \left(1+\frac{\gamma_N}{\gamma_S \mathcal{J}} n\right)}{1+\frac{\gamma_P}{\gamma_C}(I-1)} \left(1 - \frac{\gamma_P I}{\gamma_C \left(1+\frac{\gamma_P}{\gamma_C}(I-1)\right)} \right) \right] \\
&\quad - \Delta^2 \lambda \left[\frac{I \frac{\gamma_N}{\gamma_S}}{1+\frac{\gamma_P}{\gamma_C}(I-1)} + 1 \right] + (1-K)\lambda\epsilon\Delta\Gamma_\tau - \mu\Gamma_\tau^2 \\
&= \Gamma^2 \left[-I \left(1+\frac{\gamma_N}{\gamma_S \mathcal{J}} n\right) \frac{\gamma_P}{\gamma_S} \left(\frac{1}{1+\frac{\gamma_P}{\gamma_C}(I-1)} - \frac{\gamma_C}{2I\gamma_P} \right)^2 \right. \\
&\quad \left. + \frac{\gamma_C^2}{4I\gamma_P\gamma_S} \left(1+\frac{\gamma_N}{\gamma_S \mathcal{J}} n\right) - \frac{\gamma_C}{\gamma_S} + \mu \right] \\
&\quad + \Gamma\Delta \left(\frac{1}{1+\frac{\gamma_P}{\gamma_C}(I-1)} \right) \\
&\quad \left[\frac{\gamma_C \gamma_N I}{\gamma_S^2 \mathcal{J}} - \lambda \mathcal{J} \left(1+\frac{\gamma_N}{\gamma_S \mathcal{J}} n\right) \left(1 - \frac{\gamma_P I}{\gamma_C \left(1+\frac{\gamma_P}{\gamma_C}(I-1)\right)} \right) \right] \\
&\quad - \Delta^2 \lambda \left[\frac{I \frac{\gamma_N}{\gamma_S}}{1+\frac{\gamma_P}{\gamma_C}(I-1)} + 1 - \frac{(1-K)^2 \epsilon^2 \lambda}{4\mu} \right] - \mu \left(\Gamma_\tau - \frac{(1-K)\epsilon\lambda}{2\mu} \Delta \right)^2 .
\end{aligned}$$

Rewrite the above equation as

$$\dot{V} = A\Gamma^2 - B\Gamma\Delta - C\Delta^2 - \mu \left(\Gamma_\tau - \frac{(1-K)\epsilon\lambda}{2\mu} \Delta \right)^2 \tag{4.3.1}$$

Note that $\dot{V}$ is not necessarily negative, since A is not necessarily negative, and the last term becomes zero when $K=1$ and $\Gamma_\tau = 0$.

4.3.1 A brute force approach Let us try to force $\dot{V}$ to be negative, and see what eventuates.

Complete the square to get

$$\dot{V} = -C \left(\Delta + \Gamma \frac{B}{2C} \right)^2 + \Gamma^2 \left(A + \frac{B^2}{4C} \right) - \mu \left(\Gamma_\tau - \frac{(1-K)\epsilon\lambda}{2\mu} \Delta \right)^2 .$$

Thus we just want the following inequalities to be satisfied:

$$C > 0 \tag{4.3.2}$$

$$\Gamma^2 \left(A + \frac{B^2}{4C} \right) - \mu \left(\Gamma_\tau - \frac{(1-K)\epsilon\lambda}{2\mu} \Delta \right)^2 < 0 \tag{4.3.3}$$

Inequality 4.3.2 We would like to force the following to be true:

$$\lambda \left[\frac{I \frac{\gamma_N}{\gamma_S}}{1 + \frac{\gamma_P}{\gamma_C}(I-1)} + 1 - \frac{(1-K)^2 \epsilon^2 \lambda}{4\mu} \right] > 0$$

The worst case scenario is where $I \approx 0$, and taking this scenario, we get the following range for λ:

$$0 < \lambda < \frac{4\mu}{(1-K)^2 \epsilon^2} \tag{4.3.4}$$

Inequality 4.3.3 If $A + \frac{B^2}{4C} \leq 0$, then the condition is automatically satisfied. Now consider when $A + \frac{B^2}{4C} > 0$. We can factorise inequality (4.3.3) to give

$$\left(|\Gamma| \sqrt{A + \frac{B^2}{4C}} + \sqrt{\mu} \left| \Gamma_\tau - \frac{(1-K)\epsilon\lambda}{2\mu} \Delta \right| \right) \left(|\Gamma| \sqrt{A + \frac{B^2}{4C}} - \sqrt{\mu} \left| \Gamma_\tau - \frac{(1-K)\epsilon\lambda}{2\mu} \Delta \right| \right) < 0$$

Note that the first bracketed term is non-negative, so we need the second bracketed term to be negative to satisfy the inequality; that is, we need

$$|\Gamma| \sqrt{A + \frac{B^2}{4C}} - \sqrt{\mu} \left| \Gamma_\tau - \frac{(1-K)\epsilon\lambda}{2\mu} \Delta \right| < 0. \tag{4.3.5}$$

Rewrite A, B, C to show their dependence on μ, λ, K:

$$\begin{aligned} A &= A_1 + \mu \\ B &= B_1 + B_2 \lambda \\ C &= C_1 \lambda + C_2 \frac{\lambda^2}{\mu}(1-K)^2 \end{aligned}$$

Inequality 4.3.5 now becomes

$$|\Gamma| \sqrt{A_1 + \mu + \frac{(B_1 + B_2\lambda)^2 \mu}{4(C_1\lambda + C_2\frac{\lambda^2}{\mu}(1-K)^2)}} - \sqrt{\mu} \left| \Gamma_\tau - \frac{(1-K)\epsilon\lambda}{2\mu} \Delta \right| < 0 \tag{4.3.6}$$

The complete coupling case Consider the case when $K = 1$, when we would expect the strongest synchronisation to occur. Inequality (4.3.6) reduces to

$$|\Gamma| \sqrt{A_1 + \mu + \frac{(B_1 + B_2\lambda)^2 \mu}{4C_1\lambda}} - \sqrt{\mu} |\Gamma_\tau| < 0 \tag{4.3.7}$$

Since C_1 is always positive, we want $\frac{(B_1+B_2\lambda)^2\mu}{\lambda}$ to be as small as possible, so let us optimise with respect to λ. A local minimum will occur when

$$\lambda = \left| \frac{B_1}{B_2} \right|$$

Note that B_1 is positive for sensible values of I and B_2 is negative for $n > -\frac{\gamma_S \mathcal{J}}{\gamma_N}$, which happens to include all simulated values of n. This forces $(B_1 + B_2\lambda)$ to be zero, which reduces condition 4.3.7 to

$$|\Gamma|\sqrt{A_1 + \mu} - \sqrt{\mu}|\Gamma_\tau| < 0 \tag{4.3.8}$$

From this we can see that there are two cases:

- if $A_1 \leq 0$, we can set $A_1 + \mu$ to be as small as we like, and so the condition is satisfied (note that μ can vary in a continuous manner to do this because A_1 is continuous)
- if $A_1 > 0$, the best we can do is to set μ as large as possible, and have $|\Gamma_\tau| > |\Gamma|$

Let us look at when $A_1 > 0$:

$$A_1 = \frac{\gamma_C}{\gamma_S}\left(\frac{1 + \frac{\gamma_N}{\gamma_S \mathcal{J}}n}{1 + \frac{\gamma_P}{\gamma_C}(I-1)} - 1\right) - \frac{\gamma_P}{\gamma_S}I\left[\frac{1 + \frac{\gamma_N}{\gamma_S \mathcal{J}}n}{\left(1 + \frac{\gamma_P}{\gamma_S}(I-1)\right)^2}\right] > 0$$

Since, for reasonable I, $1 + \frac{\gamma_P}{\gamma_C}(I-1) > 0$, we want to know when

$$-\frac{\gamma_C}{\gamma_S}\left(1 + \frac{\gamma_P}{\gamma_C}(I-1)\right)^2 + \frac{\gamma_C}{\gamma_S}\left(1 + \frac{\gamma_N}{\gamma_S \mathcal{J}}n\right)\left(1 + \frac{\gamma_P}{\gamma_C}(I-1)\right) - \frac{\gamma_P}{\gamma_S}I\left(1 + \frac{\gamma_N}{\gamma_S \mathcal{J}}n\right) > 0$$

This simplifies to

$$-\frac{\gamma_C}{\gamma_S}\left(1 + \frac{\gamma_P}{\gamma_C}(I-1)\right)^2 + \left(1 + \frac{\gamma_N}{\gamma_S \mathcal{J}}n\right)\left(\frac{\gamma_C - \gamma_P}{\gamma_S}\right) > 0$$

Figure 4.3.1 shows the area of phase space where A_1 is positive. When the system falls into the region of phase space

$$\{(I,n) : A_1 \leq 0\} \cup \{(I,n) : A_1 \geq 0 \text{ and } |\Gamma_\tau| > |\Gamma|\}$$

we can guarantee that the two systems will be actively synchronising.

4.3.2 A second approach The previous approach gained us some information, but has not successfully proven synchronisation of the two laser systems. Let us go back to equation 4.3.1:

$$\dot{V} = A\Gamma^2 - B\Gamma\Delta - C\Delta^2 - \mu\left(\Gamma_\tau - \frac{(1-K)\epsilon\lambda}{2\mu}\Delta\right)^2$$

We will consider the complete coupling case, $K = 1$. At any moment of time, we can write Γ_τ as a multiple of Γ in the following way:

$$\Gamma_\tau = \Gamma\delta$$

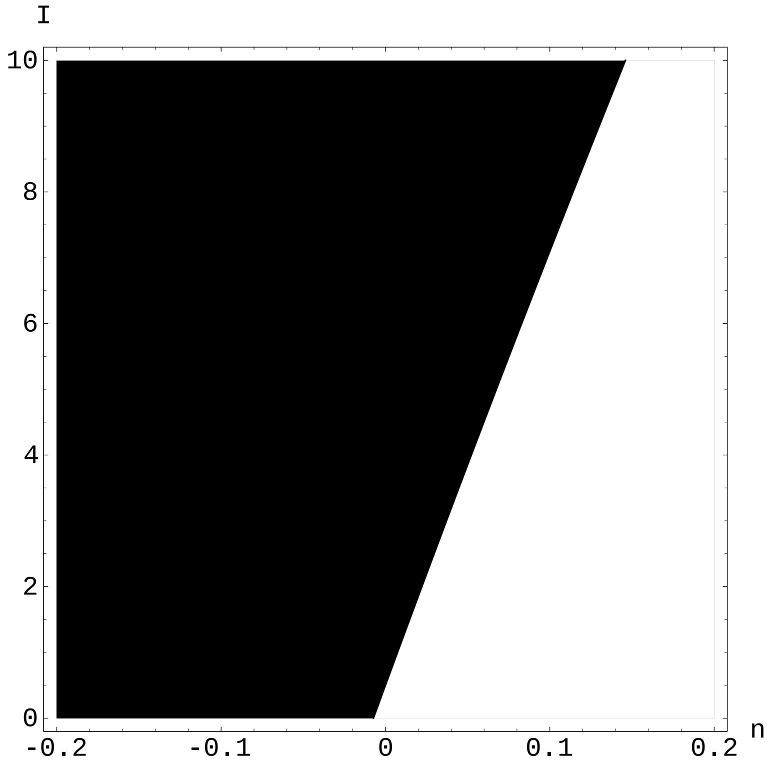

Figure 4.3.1: The white part is the area of phase space where A_1 is positive, while the black part is the area of phase space where A_1 is non-positive.

$$\dot{V} = (A-\mu)\delta\Gamma^2 - B\Gamma\Delta - C\Delta^2$$

If $(A-\mu)\delta < 0$ and $C > 0$, we can complete the square to get

$$\begin{aligned}
\dot{V} &= -(\mu - A)\delta\left(\Gamma^2 + \frac{B}{(\mu-A)\delta}\Gamma\Delta + \frac{C}{(\mu-A)\delta}\Delta^2\right) \\
&= -(\mu - A)\delta\left(\Gamma + \sqrt{\frac{C}{(\mu-A)\delta}}\Delta\right)^2 \\
&\quad + \left(\frac{B}{(\mu-A)\delta} - 2\sqrt{\frac{C}{(\mu-A)\delta}}\right)\Gamma\Delta
\end{aligned}$$

If we set μ large enough, then $\dot{V} < 0$. Note that the assumption $C > 0$ (which was dealt with previously in section 4.3.1) is always true when $K = 1$. Also note that this analysis only requires

$$\delta > 0$$

or, in other words, that Γ and Γ_τ be the same sign.

Thus, in addition to the previous region, we now know that the systems will synchronise if Γ and Γ_τ have the same sign. At all other times, our analysis of the Lyapunov function gives us little useful information. In the worst case, the two systems may be actively desynchronising. This may not be such a problem if the two systems do not desynchronise too much. This may occur either because they do not spend much time in the problematic region, or because they may not desynchronise quickly when they are in the problematic region.

The next chapter will show numerical simulations of the semiconductor laser system, and demonstrate what the above analyses tell us about our simulations.

Numerical results for the semiconductor laser

5.1 Simulations

This section contains the results from numerical simulations of the semiconductor equations. To numerically integrate delay differential equations, the package *dde23* was used within MATLAB. The MATLAB code to simulate the semiconductor laser equations is found in Appendix A.

Figures 5.1.1 and 5.1.3 show the variables I and n respectively for a free-run. A constant history function was used for both I and n. In the figures, we can see how the artefact of a constant history disappears with time in both variables.

Figure 5.1.5 shows the area of phase space that the free-running system fills from $t = 1800$ to $t = 2000$. Note that the system spends a significant amount of time in the (possibly) problematic region, $A_1 > 0$.

After running two systems uncoupled long enough to lose the constant history artifact, they are coupled together with a full coupling ($K = 1$). Figure 5.1.6 shows the difference in I between the two uncoupled systems, while figure 5.1.8 shows the difference in I between the systems after coupling. Note how quickly the two systems synchronise after coupling. Figure 5.1.9 shows that the error system (Γ, Δ) passes close to the origin periodically when the two systems are uncoupled.

5.2 Analysis of simulation results

We want to relate the numerical simulations to our analysis, and so we will calculate

$$\int_{t-10}^{t} |\Gamma(\theta)|^2 d\theta$$

which is the part of the Lyapunov function that guarantees uniform asymptotic stability. To show robust synchronisation, we need this part to be monotone decreasing. As expected, figures 5.2.1 and 5.2.2 show that the integral is not monotone decreasing when there is no coupling between the systems.

After coupling, figure 5.2.3 shows that numerically, the function appears to be monotone decreasing, except for a small section just after the systems are coupled together, when we would not expect our linearisation to be valid (see figure 5.2.4).

Figures 5.2.5, 5.2.6 and 5.2.7 show when each analysis is valid; in order, they are

- $A_1 \leq 0$
- $|\Gamma_\tau| > |\Gamma|$
- Γ and Γ_τ are the same sign

Figure 5.2.8 shows these graphs superimposed. There are only a few data points near the beginning of the graph that do not fall into one of these regions. Note that the second condition almost always ensures that the systems continue to synchronise once they have started to do so, which may preclude the need for synchronisation of the strongest kind.

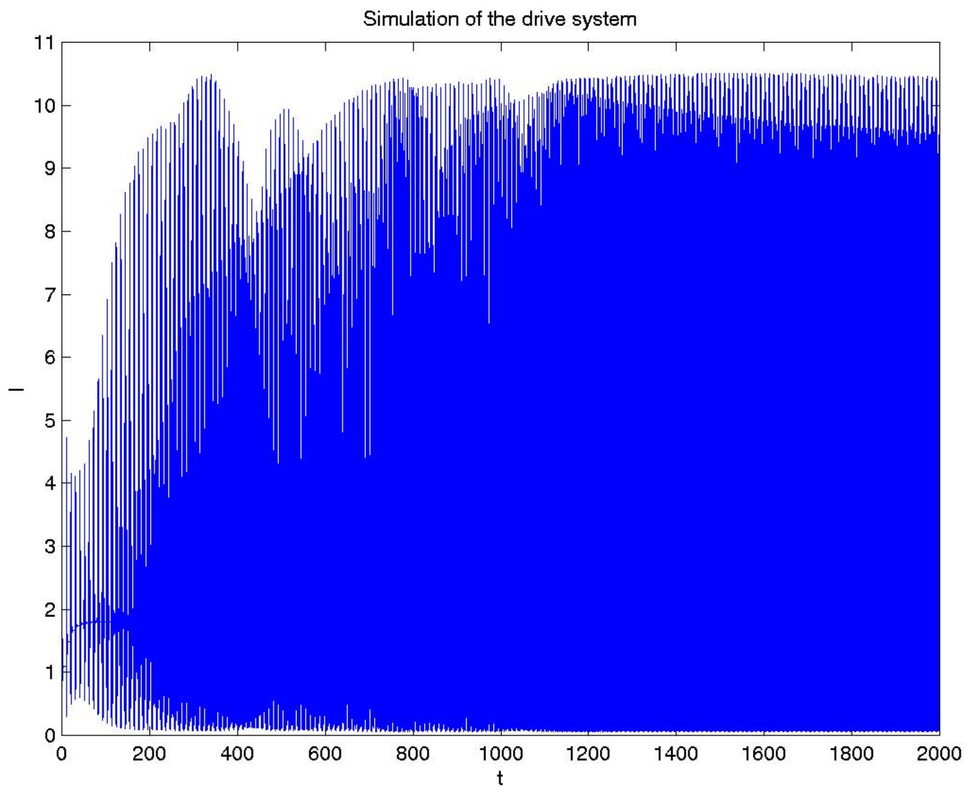

Figure 5.1.1: Intensity of the drive system from $t = 0$ to $t = 2000$

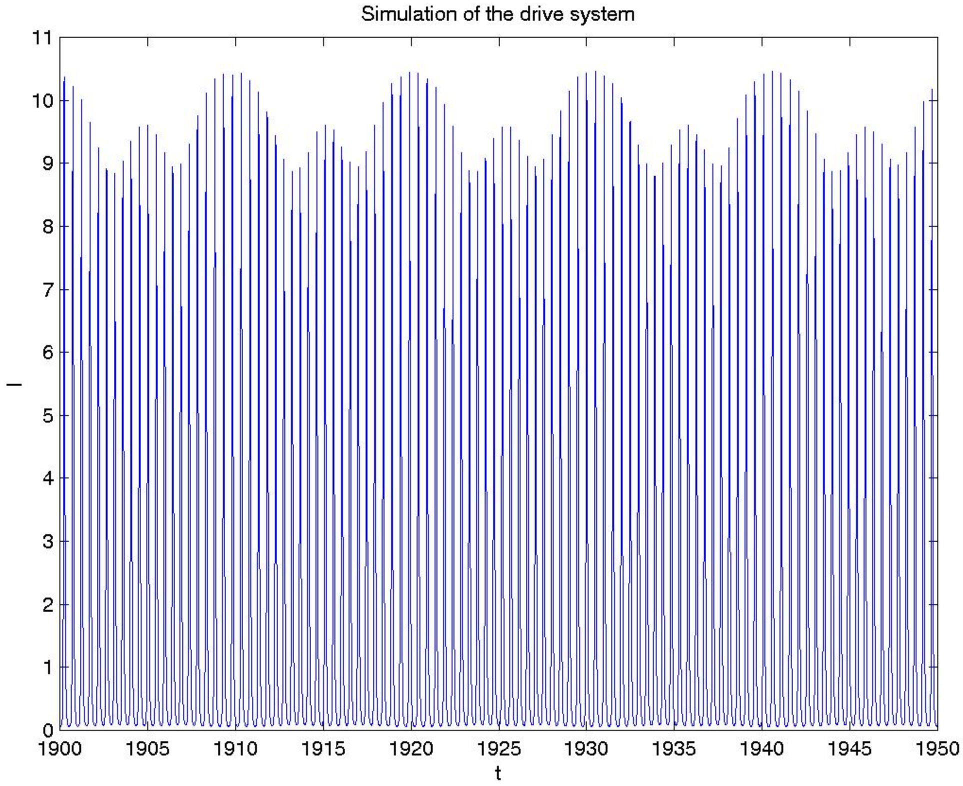

Figure 5.1.2: Enlargement of figure 5.1.1, showing domain $t = 1900$ to $t = 1950$

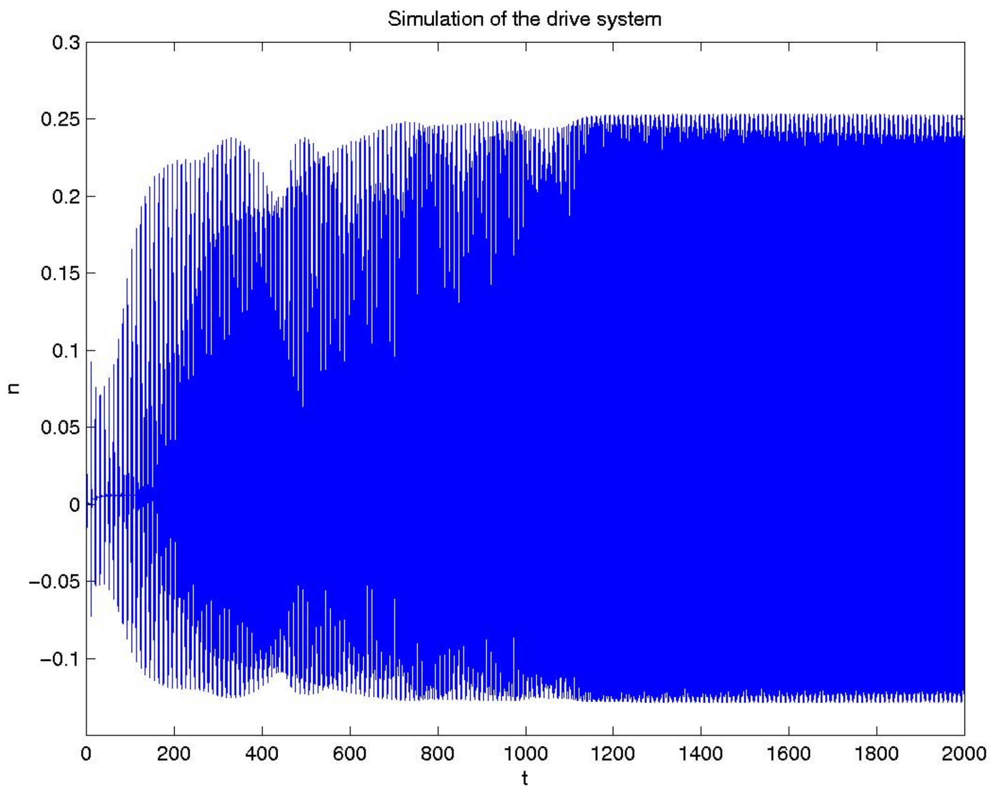

Figure 5.1.3: Population inversion of the drive system from $t = 0$ to $t = 2000$

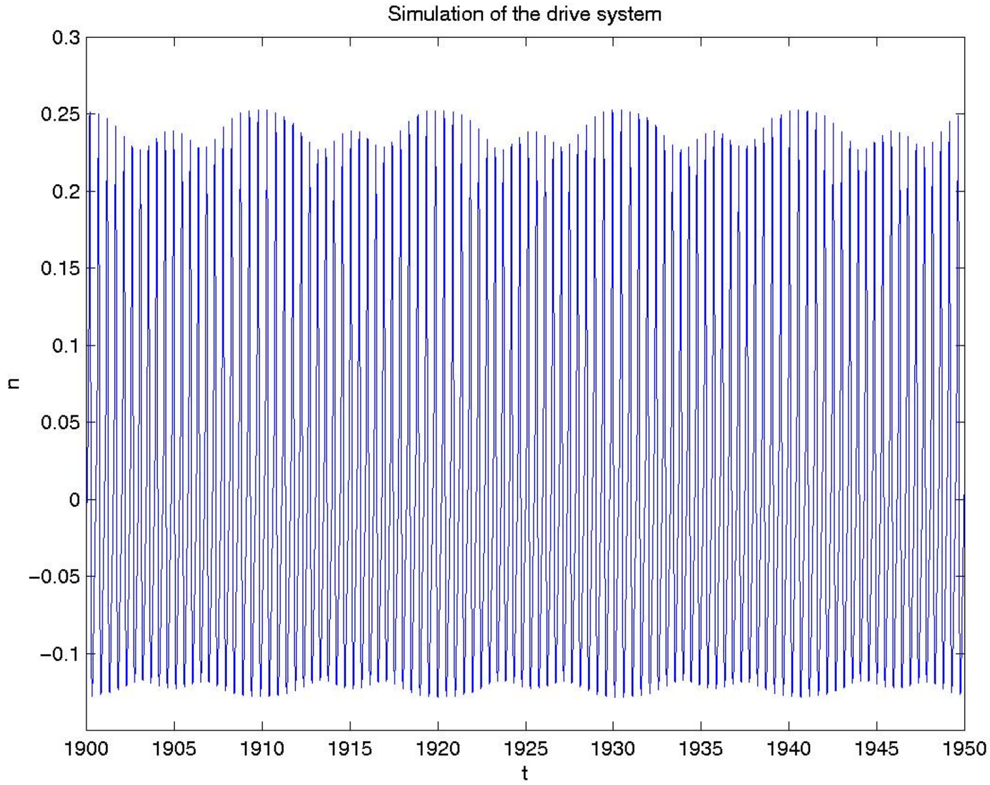

Figure 5.1.4: Enlargement of figure 5.1.3, showing domain $t = 1900$ to $t = 1950$

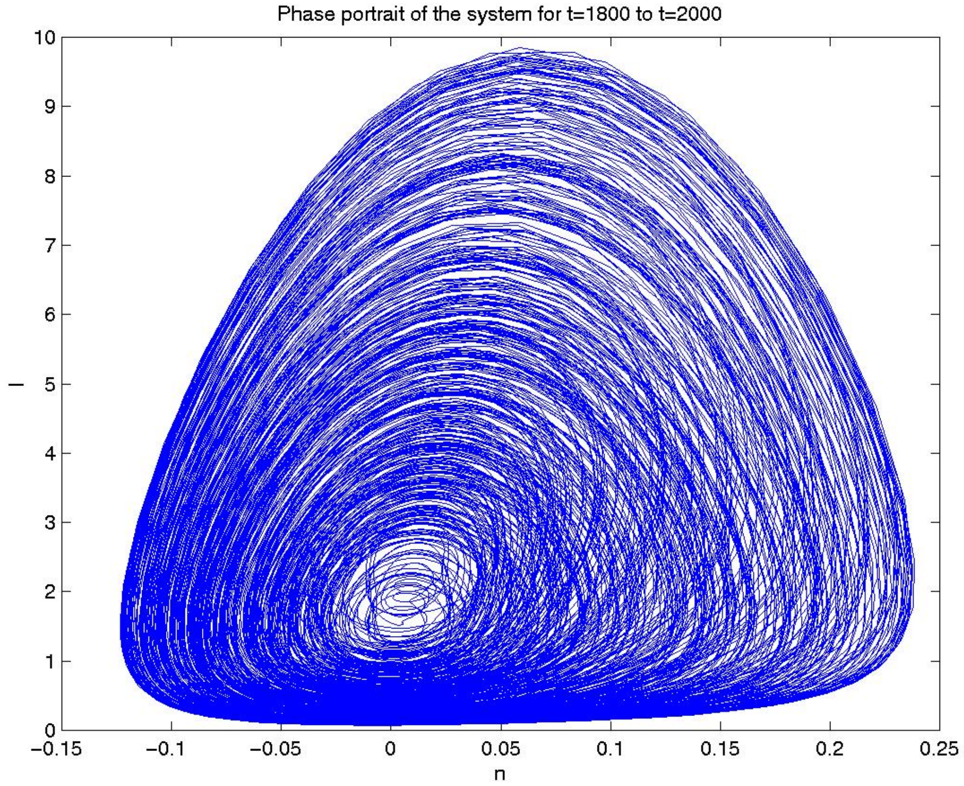

Figure 5.1.5: Phase portrait of an uncoupled system from t=1800 to t=2000

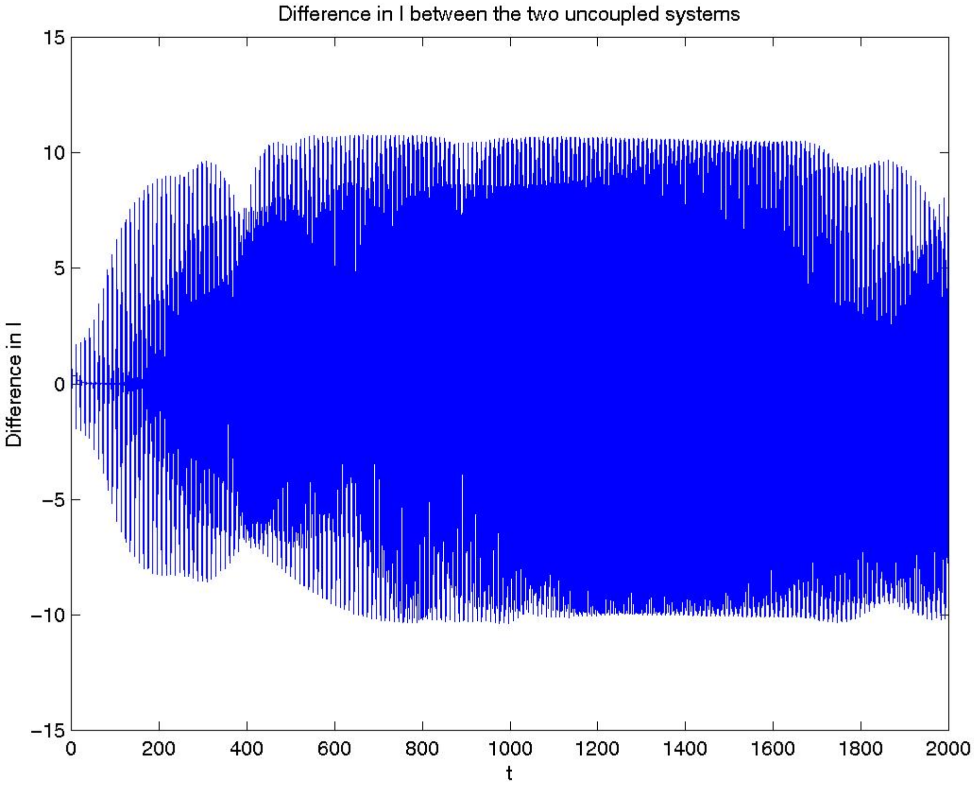

Figure 5.1.6: Difference in intensity of the two uncoupled systems

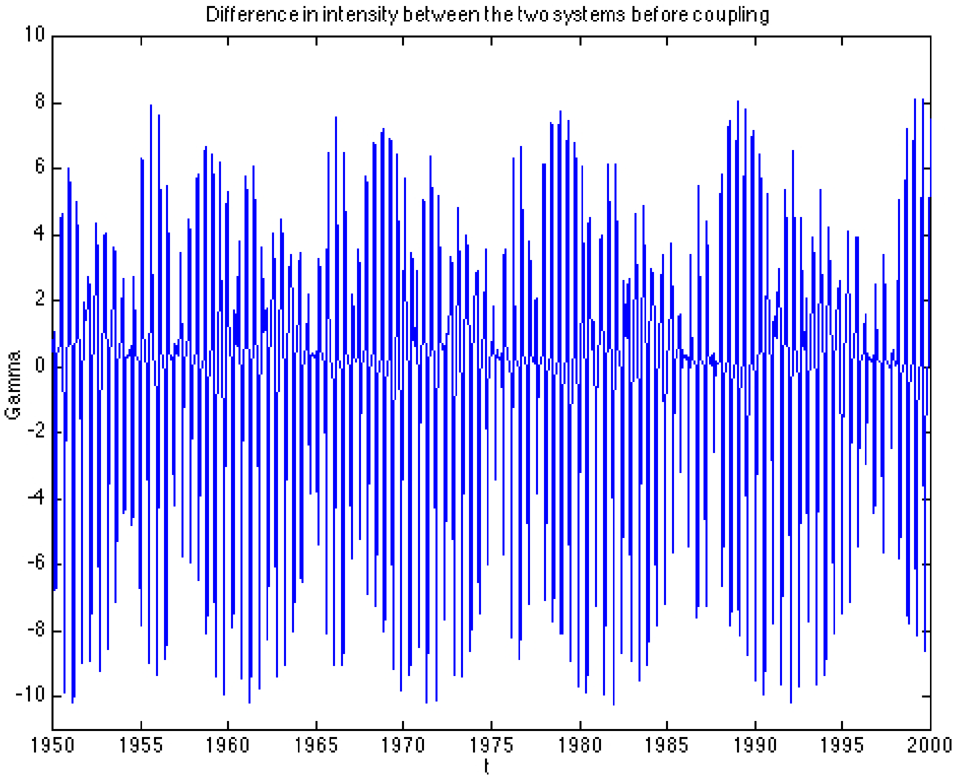

Figure 5.1.7: Enlargement of figure 5.1.6, showing domain $t = 1950$ to $t = 2000$

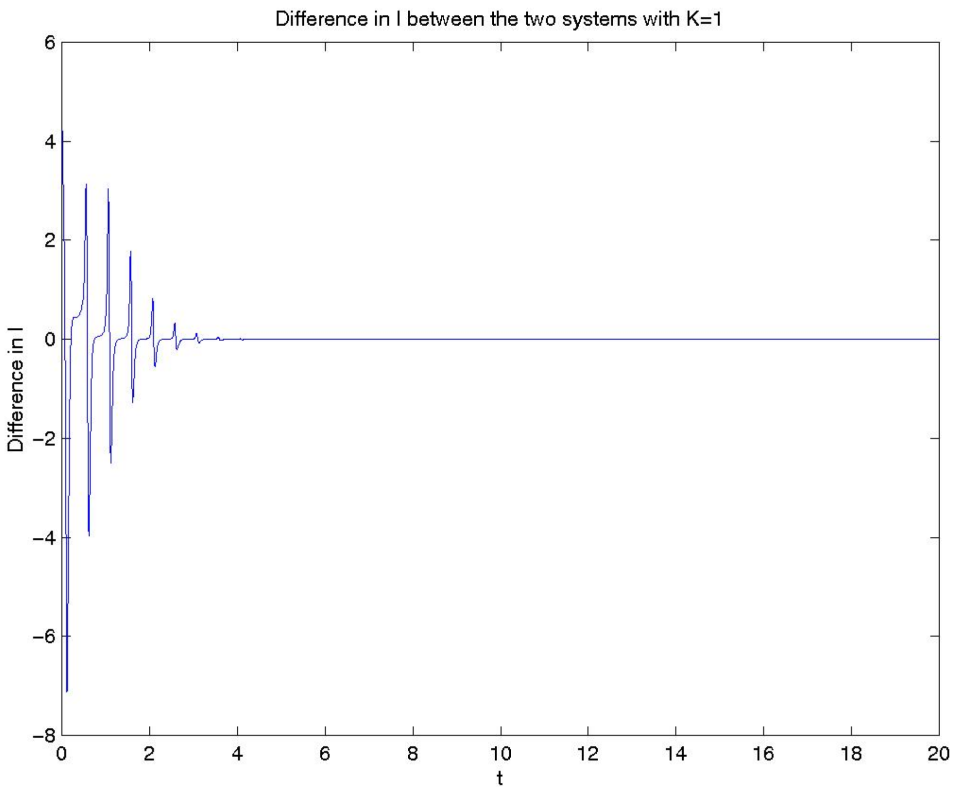

Figure 5.1.8: Difference in intensity of the two systems after coupling

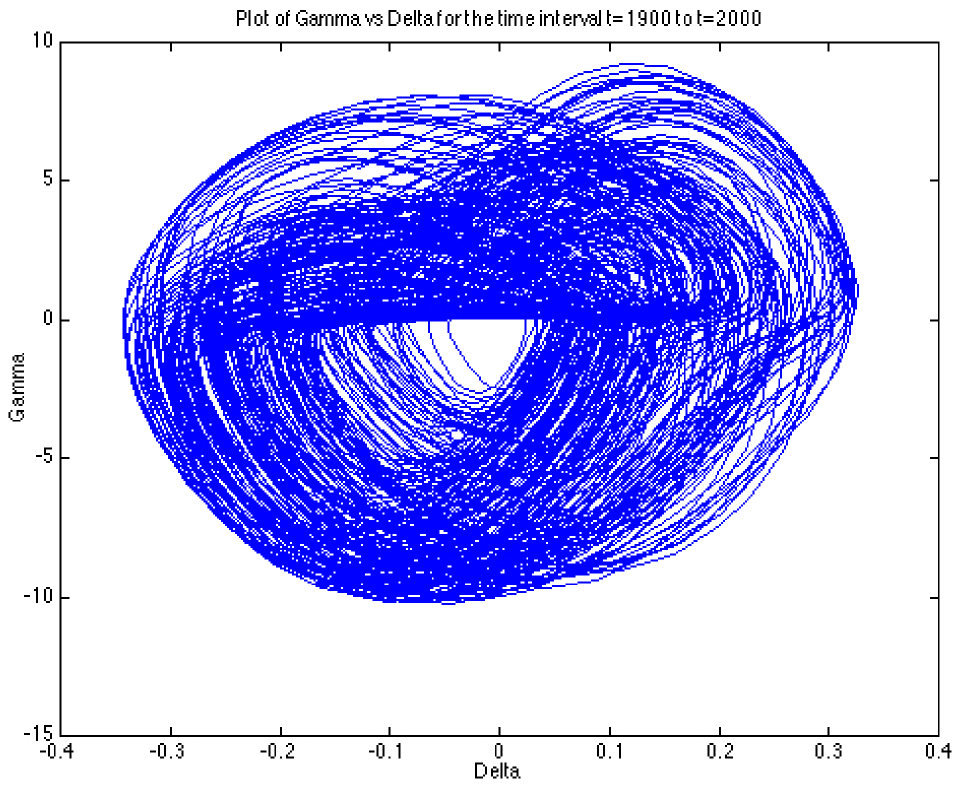

Figure 5.1.9: Graph of Γ vs Δ over the time period $t = 1900$ to $t = 2000$

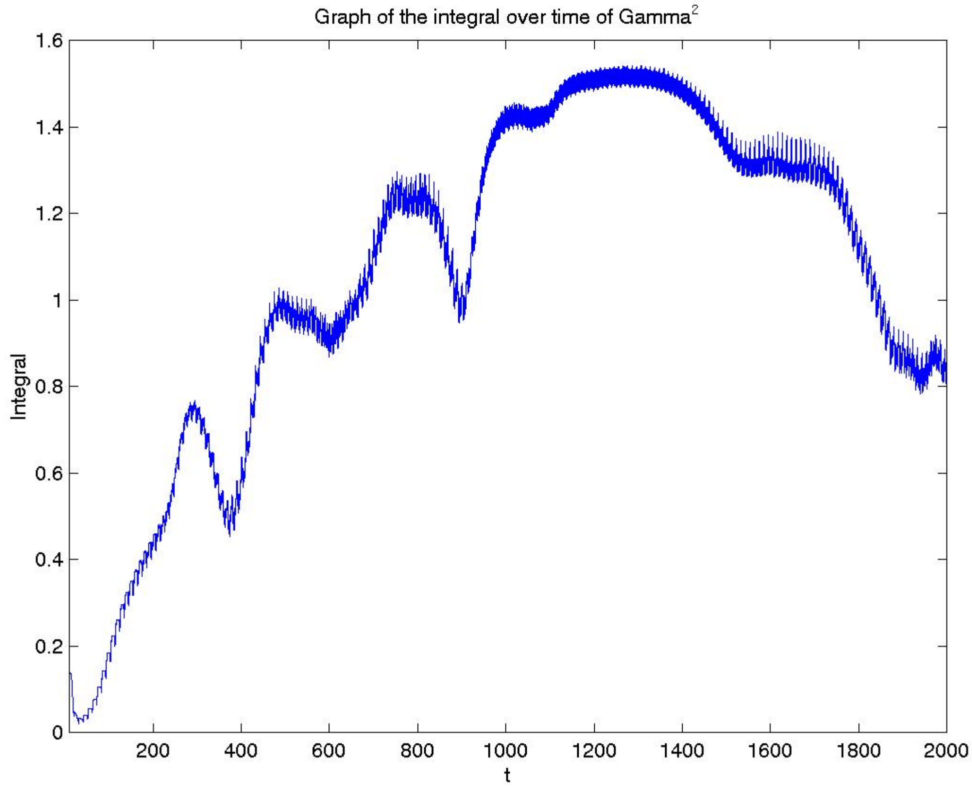

Figure 5.2.1: Graph of $\int_{t-10}^{t} |\Gamma(\theta)|^2 d\theta$ for two uncoupled systems from $t = 0$ to $t = 2000$

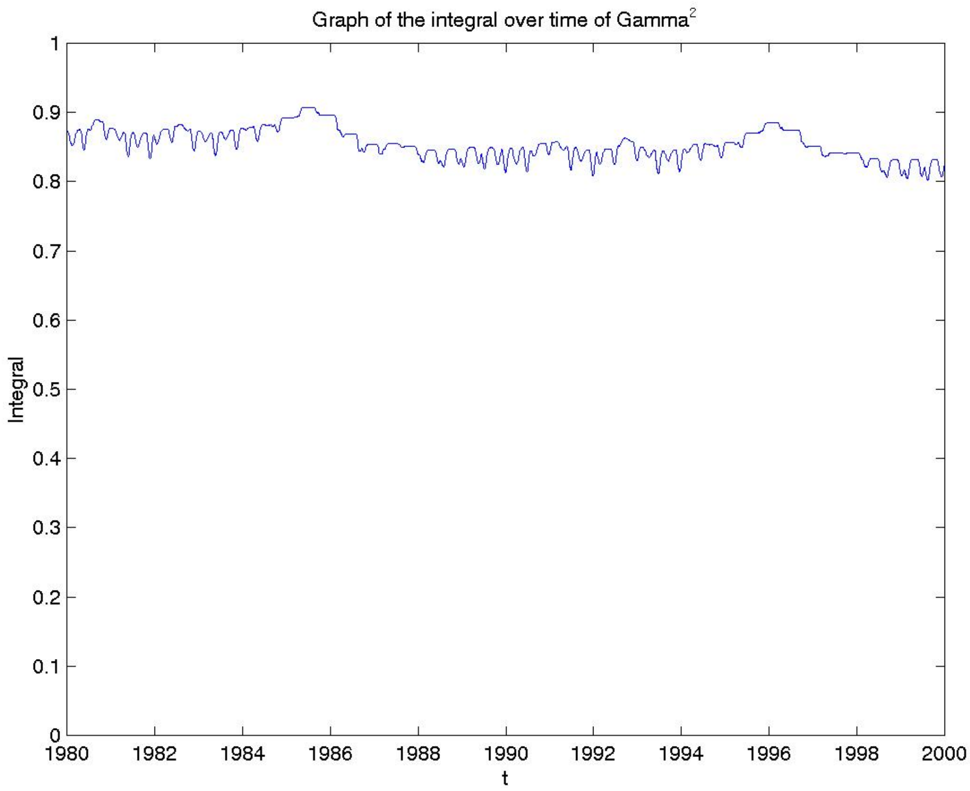

Figure 5.2.2: Enlargement of figure 5.2.1, showing domain $t = 1980$ to $t = 2000$

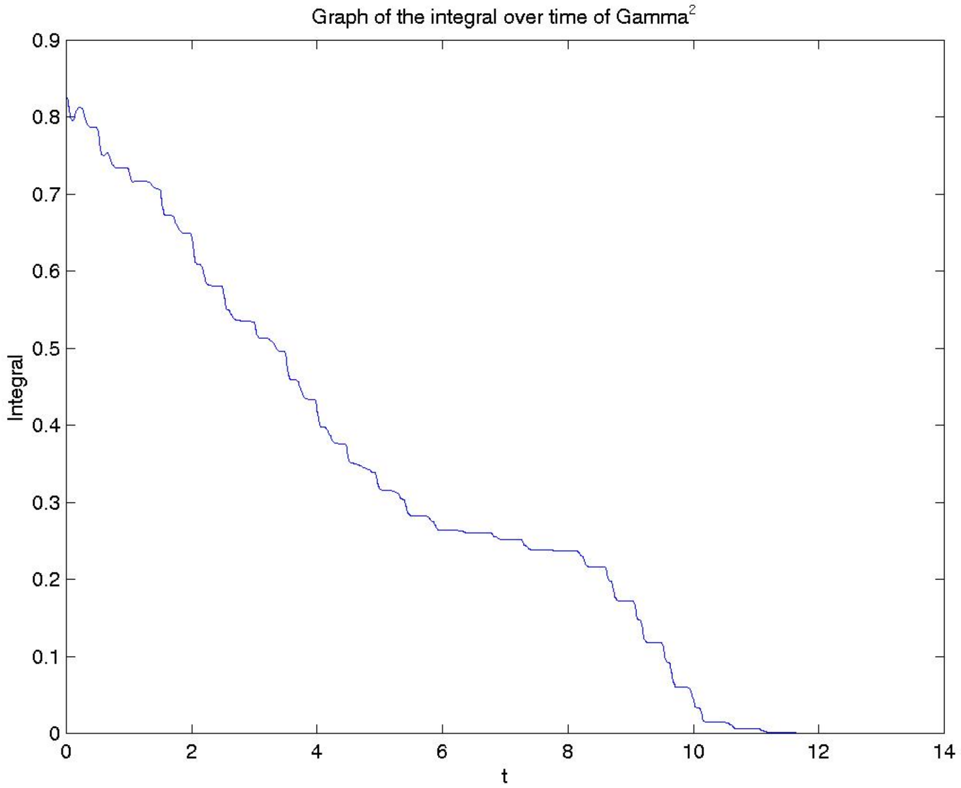

Figure 5.2.3: Graph of $\int_{t-10}^{t} |\Gamma(\theta)|^2 d\theta$ after coupling the two systems.

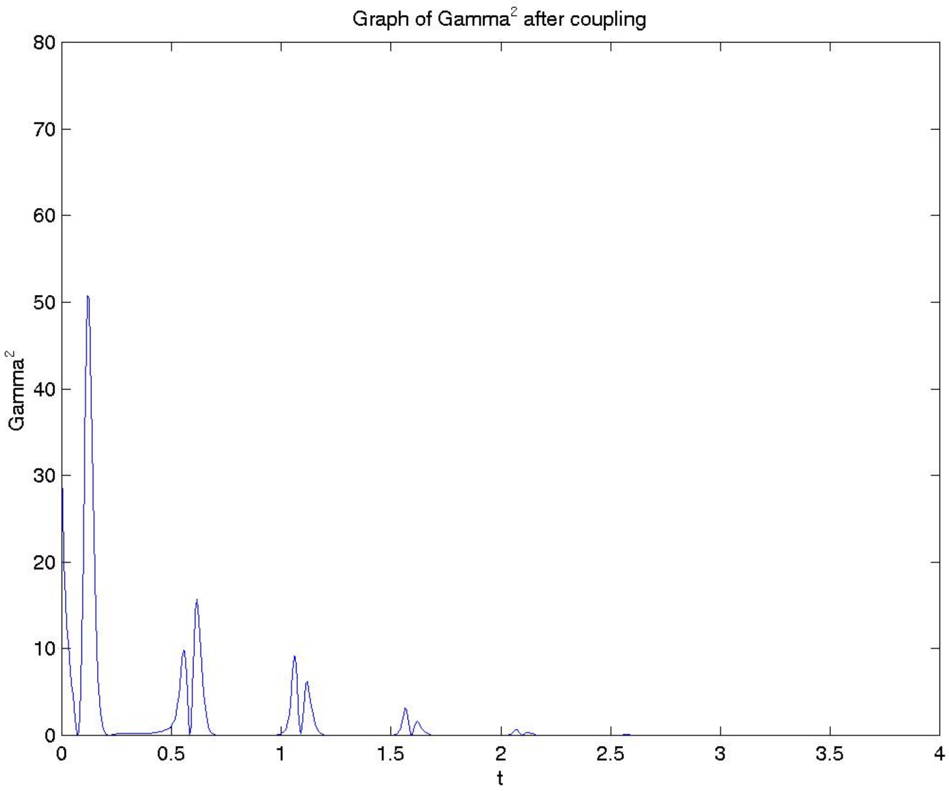

Figure 5.2.4: Graph showing Γ^2 just after coupling the two systems together

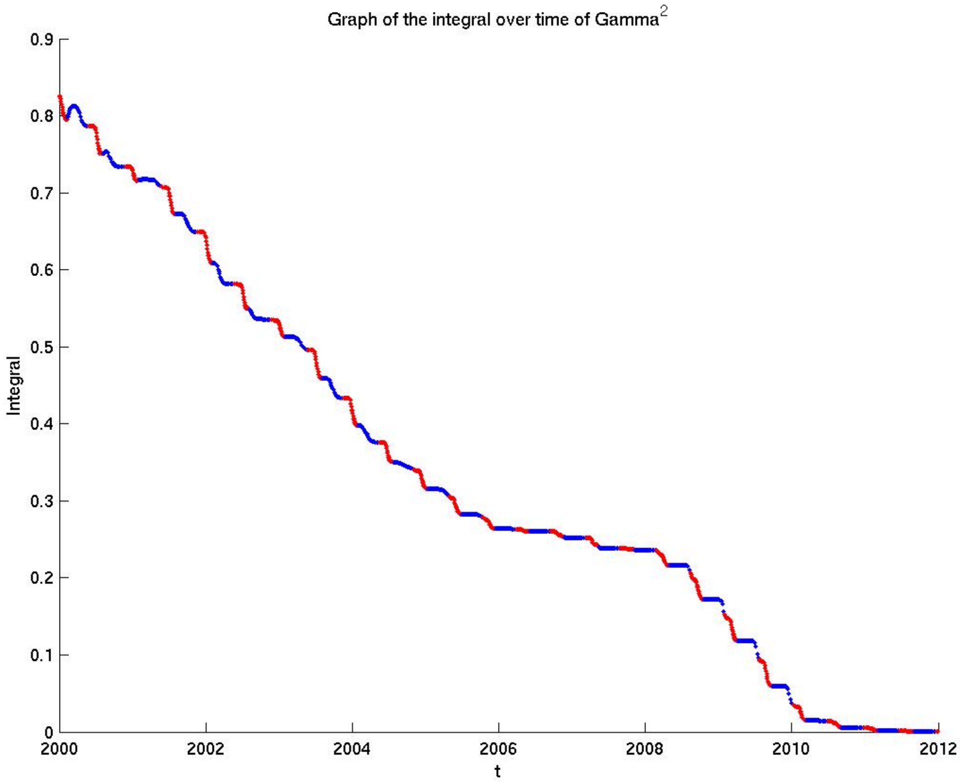

Figure 5.2.5: Graph of $\int_{t-10}^{t} |\Gamma(\theta)|^2 d\theta$ after coupling the two systems. The graph is blue when $A_1 \leq 0$, and red at all other times.

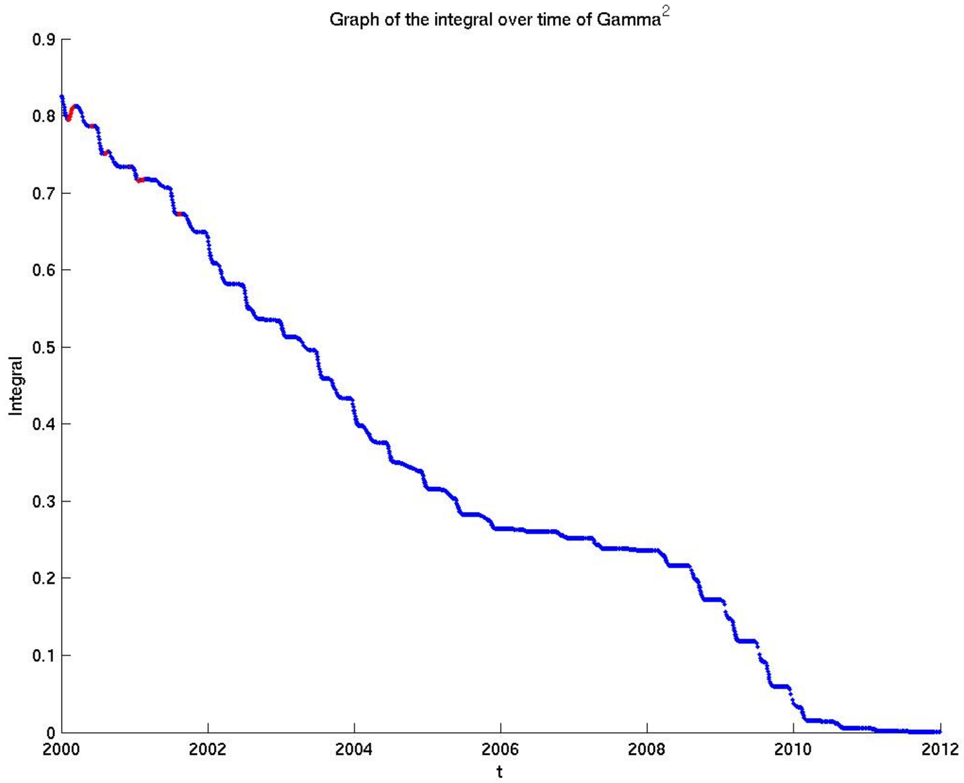

Figure 5.2.6: Graph of $\int_{t-10}^{t} |\Gamma(\theta)|^2 d\theta$ after coupling the two systems. The graph is blue when $|\Gamma_\tau| > |\Gamma|$, and red at all other times.

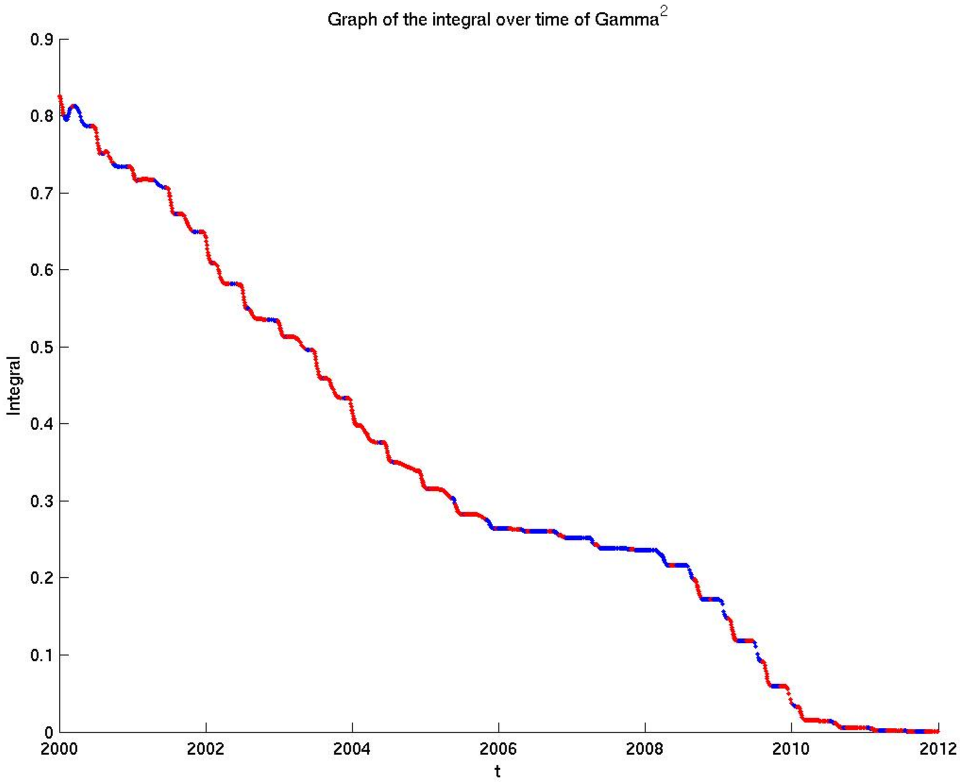

Figure 5.2.7: Graph of $\int_{t-10}^{t} |\Gamma(\theta)|^2 d\theta$ after coupling the two systems. The graph is blue when Γ_τ and Γ are the same sign, and red at all other times.

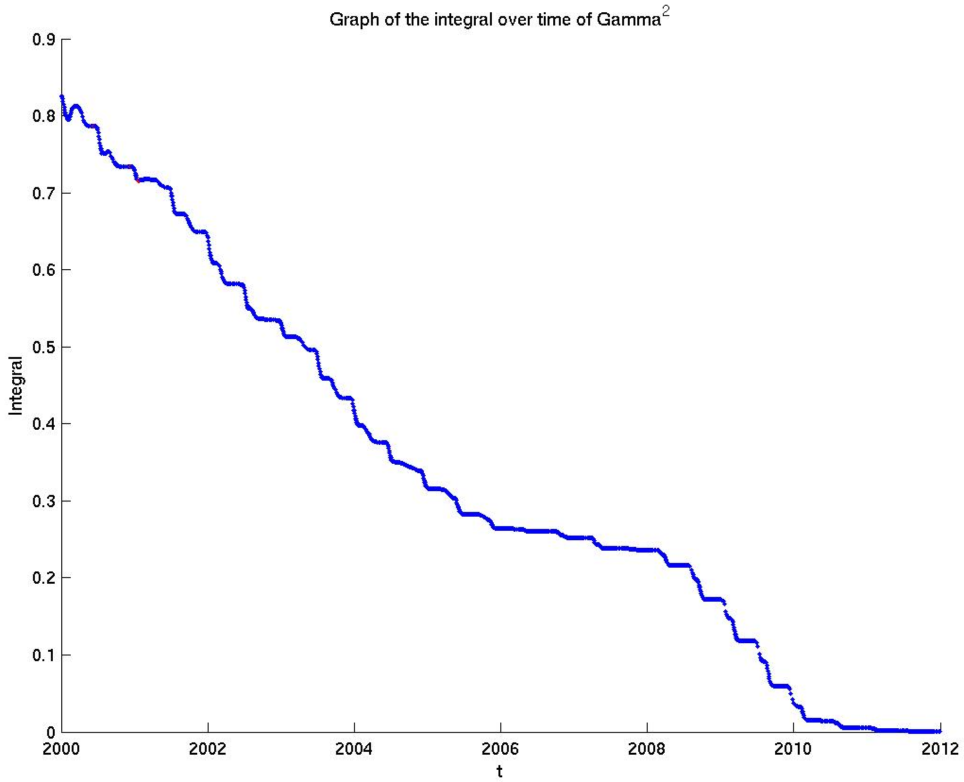

Figure 5.2.8: Graph of $\int_{t-10}^{t} |\Gamma(\theta)|^2 d\theta$ after coupling the two systems. The graph is blue when at least one condition is satisfied, and red at all other times.

Final thoughts

6.1 Conclusions

The two examples in this thesis show the application of the method of Lyapunov functions to the area of synchronisation. This method allows us to either guarantee robust synchronisation or gain insight into why robust synchronisation may not be occurring by checking a sufficient condition. Not surprisingly, this sufficient condition is more difficult to check than the necessary condition of negative conditional Lyapunov exponents, since the multipliers in front of each term in the Lyapunov function need to be adjusted.

In the first example, the method was applied successfully, and a range of coupling is established analytically under which robust synchronisation is guaranteed. Numerically, we could show robust synchronisation for a larger range of coupling and without the need to linearise around the origin of the error system, by checking out when $\dot{V}$ can be made negative by an appropriate choice of multipliers.

The second example showed the method of Lyapunov functions applied in an less successful manner. This could be because the choice of Lyapunov function was inappropriate, or because robust synchronisation does not actually occur. However, the standard choice of Lyapunov function gave us some insight into what sort of synchronisation behaviour we would expect from the coupled systems. Our simulation results give us some measure of confidence that the general tendency of the systems is to synchronise when given a complete coupling.

However, if we observe desynchronisation in simulations or experiments, we could investigate (numerically) how $\dot{V}$ could be minimised when positive by appropriate choices of multipliers, so that we get some estimate of the maximum rate of desynchronisation possible. We could also find out what rate of synchronisation is guaranteed when $\dot{V}$ is negative. If on average, we can show numerically that the tendency of the coupled systems is to synchronise, but that robust synchronisation does not occur at all times, this may allow us to alter the behaviour of the system or the coupling regime to improve synchronisation or reduce the frequency or rate of desynchronisation.

6.2 Further work

At present, the analytic study of each individual system is an involved process, without a well-defined method. In a lot of ways, the process seems rather hit-and-miss, with reasonably arbitrary combinations of terms to try to force the expression $\dot{V}$ to be negative. In addition, the method may not provide sufficient insight to justify the time required to apply it. A study of the results given by numerical methods would be useful to show whether they can be applied more readily to other problems.

The more difficult problem of synchronisation in the presence of message transfer needs more work. This will depend on factors such as the size and shape of the waveform used to transmit the message. Radically different methods may well be necessary to address this problem analytically.

Appendix A – MATLAB code

The package *dde23* was used to simulate the delay differential equations in MATLAB. The following subsections contain the MATLAB code that was used.

A.1 Code used to simulate the equations

This code was split into the two files `simulate.m` and `equations.m` which respectively contain the *dde23* function call and the system of equations.

The following code simulates two coupled systems with coupling constant `K`.

`simulate.m`

```
sol = dde23('equations',10,[0.2,0.2,1.0,0.1],[0,2000]);
%In order, this function call:
% - reads the system of equations from 'equations.m'
% - sets the time lag to 10
% - gives the first system a constant history function of
%   (I,n) = (0.2,0.2)
% - gives the second system a constant history function of
%   (I,n) = (1.0,0.1)
% - specifies that a solution is required from t = 0 to 2000
%The output sol contains a lot of information. Two parts of sol are
%especially important:
% - sol.x is a vector containing the times at which the numerical
%   integrator evaluated the differential equations
% - sol.y is a matrix containing four vectors representing the
%   variables y(1), y(2), y(3), y(4) as defined in equations.m
```

`equations.m`

```
function v = semi_f(t,y,Z)
% - t is the time variable
% - y(1) and y(2) are the I and n variables from the first system
% - y(3) and y(4) are the I and n variables from the second system
% - Z(1) and Z(3) are the delayed I variables from the first and
%   second system respectively
% - v is the time derivative of y
v = zeros(4,1);

v(1) = (240/1.458)*(((1+(2/1.458)*y(2))/(1+0.01*(y(1)-1)))-1)*y(1);
v(2) = (2/3)*(1-((1+(2/1.458)*y(2))/1+0.01*(y(1)-1)))*y(1))-y(2)
                                                      +0.3*Z(1);
v(3) = (240/1.458)*(((1+(2/1.458)*y(4))/(1+0.01*(y(3)-1)))-1)*y(3);
v(4) = (2/3)*(1-((1+(2/1.458)*y(4))/1+0.01*(y(3)-1)))*y(3))-y(4)
                                          +0.3*(K*Z(1)+(1-K)*Z(3));
```

A.2 Code used to generate the single-colour integral plot

The following code plots the integral of Γ^2 from `t - tau` to `t`. The starting point function value in the Riemann sum has been linearly interpolated. Note that `tau` is set to 10 in our analysis.

integral.m

```
% - datasize is the number of data points in the numerical solution
datasize = size(sol.x,2);
% - weighted_sq takes into account the different spacing of the
%   data points in time
weighted_sq = ((sol.y(3,1:datasize - 1)-sol.y(1,1:datasize - 1))
                                                .*diff(sol.x)).^2;
count = 1;
start = min(find(sol.x >= tau));

% The following code takes data point i and searches for the
% closest data points to i-10. An approximation to the value of the
% function at the left hand end point is found by linear
% interpolation, and then the integral is calculated as a Riemann
% sum.
for i = start : datasize - 1
  for j = count : i
    if sol.x(j) >= sol.x(i) - tau
      if j ~= 1
        int(i) = sum(weighted_sq(j:i-1))
                        +weighted_sq(j-1)*(sol.x(j)-(sol.x(i)-tau));
        count = j;
        break;
      else
        int(i) = sum(weighted_sq(1:i-1));
        break;
      end
    end
  end
end

% The following code plots the integral against time.
int1 = [0 int];
plot(sol.x,int1);
title('Graph of the integral over time of Gamma^2');
xlabel('t')
ylabel('Integral')
V = axis; Vnew = V + [tau 0 0 0]; axis(Vnew);
```

A.3 Code used to generate coloured integral plots

Here, I will give the code for the condition $A_1 \leq 0$ – the others are similar.

```
colour_Aneg.m

  start = min(find(sol.x >= 2000));
  finish = max(find(sol.x <= 2012));

  hold on;

  gC_gS = 240/1.458;
  gP_gC = 0.01;
  gN_gSJ = 1.333/(1.458*0.6667);
  gP_gS = 2.4/1.458;

  for i = start : finish
    if (-gC_gS*(1+gP_gC*(sol.y(1,i)-1))^2)
     +(1+gN_gSJ*sol.y(2,i))*(gC_gS-gP_gS)<=0
      plot(sol.x(i),int(i),'b.')
    else
      plot(sol.x(i),int(i),'r.')
    end
  end

  title('Graph of the integral over time of Gamma^2');
  xlabel('t');
  ylabel('Integral');
  axis([2000 2012 0 0.9]);
```

Bibliography

[1] H. D. I. Abarbanel and M. B. Kennel, 'Synchronizing high-dimensional chaotic optical ring dynamics', *Physical Review Letters* **80** (1998), no. 14, 3153–3156.

[2] H. D. I. Abarbanel, M. B. Kennel, and L. Illing, 'Synchronization and communication with electro-optically modulated semiconductor lasers', *Tech. Report* (Institute for Nonlinear Science, University of California, San Diego, 1999).

[3] M. Buhl (September 1999). Private communication.

[4] T. A. Burton, *Stability and periodic solutions of ordinary and functional differential equations* (Academic Press, Orlando, Florida, 1985).

[5] P. F. Curran and L. O. Chua, 'Absolute stability theory and the synchronization problem', *International Journal of Bifurcation and Chaos* **7** (1997), no. 6, 1375–1382.

[6] J. K. Hale and H. Koçak, *Dynamics and bifurcations* (Springer-Verlag, New York, 1991).

[7] J. F. Heagy, T. L. Carroll, and L. M. Pecora, 'Experimental and numerical evidence for riddled basins in coupled chaotic systems', *Physical Review Letters* **73** (1994), no. 26, 3528–3531.

[8] N. N. Krasovskiĭ, *Stability of motion. Applications of Lyapunov's second method to differential systems and equations with delay* (Stanford University Press, Stanford, California, 1963). Translated by J. L. Brenner.

[9] L. M. Pecora and T. L. Carroll, 'Synchronization in chaotic systems', *Physical Review Letters* **64** (1990), no. 8, 821–824.

[10] L. M. Pecora and T. L. Carroll, 'Driving systems with chaotic signals', *Physical Review A* **44** (1991), no. 4, 2374–2383.

[11] A. Pogromsky and H. Nijmeijer, 'Observer-based synchronization of dynamical systems', *International Journal of Bifurcation and Chaos* **8** (1998), no. 11, 2243–2254.

[12] K. Pyragas, 'Synchronization of coupled time-delay systems: Analytical estimation', *Physical Review E* **58** (1998), no. 3, 3067–3071.

[13] G. J. VanWiggeren and R. Roy, 'Communication with chaotic lasers', *Science* **279** (1998), 1198–1200.

[14] J. L. Willems, *Stability theory of dynamical systems* (Thomas Nelson, Melbourne, 1970).